To investigate the chronic effect of adiponectin in diabetic nephropathy, we used an adenovirus to chronically overexpress adiponectin in STZ-induced diabetic rats. Our results show that chronic hyperadiponectinemia induced by adenovirus-mediated gene transfer leads to improved diabetic nephropathy outcomes.

Methods

Preparation and intravenous delivery of an adenovirus expressing mouse full-length adiponectin

Adenovirus expressing mouse adiponectin (Ad-Adipo) was generated from the full-length cDNA,[10] subcloned with an AdEasy™ Adenoviral Vector System (Stratagene, La Jolla, CA, USA), propagated in HEK293 cells, and purified with Adeno-X Virus Purification and Rapid Titer Kits (Takara Bio Inc, Shiga, Japan). Control Ad-lacZ, which carries β-gal cDNA, was isolated using the same procedure.

Animal studies

Six-week-old male Wistar rats (Charles River Laboratory, Kanagawa, Japan) were housed individually under controlled light/dark (12/12 h) and temperature conditions, and had free access to water and standard rat chow. The care, use and treatment of all animals in this study were performed in accordance with the Guide for Care and Use of Laboratory Animals of the NIH and were approved by the Animal Subjects Committee of the Fukushima Medical University, Japan.

Diabetes was induced by intraperitoneal injection of STZ (80 mg/kg in 10 mmol of citrate buffer, pH 4.5) into male Wistar rats (6 weeks old). Blood glucose concentrations were measured two days after the STZ injection and monitored weekly thereafter. Only the animals with glucose concentrations higher than 350 mg/dL were considered diabetic.

Ten weeks after STZ injection, diabetic rats were injected intravenously from the tail with 0.5×10^9 p.f.u. of Ad-Adipo or Ad-lacZ per rat, as previously described.[10] As we reported previously,[10] intravenous administration of recombinant adenoviruses results in selective transgene expression in the liver. Two weeks after adenovirus injection, animals were analyzed. Twenty-hour urine was collected from each rat in individual metabolic cages and stored at −80°C after centrifugation at 2000*g* for five minutes. Urinary concentration of total protein was measured by colorimetric assays using a commercially available kit (Bio-Rad Laboratories Inc, Richmond, CA, USA).

Immunoblotting analysis

On day 14 after adenovirus injection, liver and renal cortex tissue were homogenized in liquid nitrogen and lysed in buffer containing phosphatase and protease inhibitors. After a 10-min incubation, lysates were clarified by centrifugation (10,000*g* at 4°C) and quantified for total protein. Samples of renal cortex tissue and liver tissues were separated by sodium dodecyl sulfate polyacrylamide gel electrophoresis on 12% and 20% polyacrylamide gels, respectively. Proteins of liver tissue and renal cortex tissue were transferred onto polyvinylidene fluoride membranes (Immobilon-P; Millipore, Bedford, MA, USA) and blotted with adiponectin (Affinity BioReagents, Golden, CO, USA) and TGF-β (#ab66043; Abcam, Cambridge, UK) antibodies. Membranes were then incubated with horseradish peroxidase-conjugated secondary antibodies prior to chemiluminescence detection (Pierce, Rockford, IL, USA). Band intensities were quantified by densitometry using the NIH-Image 1.6 software.

Immunohistochemistry analysis

On day 14 after adenovirus injection, the renal cortex tissues were embedded in Tissue Tec OCT Compound (Sakura Finetechnical Co, Ltd, Tokyo, Japan). Slices of 10 μm thickness were cut with a cryostat (CM1900; Leica Microsystems, Wetzlar, Germany) and collected on slides. Sections were incubated with nephrine (#ab58968; Abcam) or TGF-β (#ab66043; Abcam) antibodies. Then, sections were incubated with horseradish peroxidase-conjugated secondary antibodies. Color was developed with 3,3′-diaminobenzidine (Sigma, St Louis, MO, USA). Slices were not counterstained with hematxylin until computer image analysis was finished.

All slices were examined under a light microscope (Olympus Co, Tokyo, Japan). In each specimen, 10 random glomeruli were analyzed. All sections were examined blind.

Quantitative realtime reverse transcriptase polymerase chain reaction analysis

On day 14 after adenovirus injection, total RNA samples were extracted from the renal cortex tissues with TRIzol reagent (Invitrogen Life Technologies, Carlsbad, CA, USA), and further purified using the RNeasy kit with RNase-free DNase I treatment according to the manufacturer's instructions. Total RNA (1 μg) was reverse-transcribed with iScript cDNA Synthesis Kit according to the manufacturer's instructions (Bio-Rad Laboratories). Quantitative realtime polymerase chain reaction (PCR) was performed with a Bio-Rad system using iQ SYBR Green Supermix and specific primer pairs (Table 1) selected with Primer Express software (Applied Biosystems, Foster, CA, USA). The relative mass of specific RNAs was calculated by the comparative cycle of threshold detection method according to the manufacturer's instructions.

Analytical procedures

Plasma glucose was assayed by the glucose oxidase method (Compact Electrode Blood Sugar Analyzer Antsense; Horiba Ltd, Kyoto, Japan). Fasting plasma insulin was quantified using a rat insulin ELISA kit (Crystal Chem Inc, Chicago, IL, USA). Plasma adiponectin concentrations were determined using the Mouse/Rat Adiponectin ELISA kit (B-Bridge International Inc, San Jose, CA, USA).

Table 1 Primers used for realtime reverse transcriptase polymerase chain reaction

Target sequence	Primers	Primer sequence	Band size (bp)
Rat TGF-β1	TGFb1-674-F	5′ AATTCCTGGCGTTACCTTGG 3′	118
NM_021578	TGFb1-791-R	5′ CCTGTATTCCGTCTCCTTGG 3′	
Rat Nephrin	Nephrin-1810-F	5′ TGGGACAAGGAAGGAGAGAG 3′	199
AF172255	Nephrin-2008-R	5′ GAGGATACAGCACATTGAAGC 3′	
Rat iNOS	iNOS-1933-F	5′ ACTACTGCTGGTGGTTACAAG 3′	104
NM_012611	iNOS-2036-R	5′ AGGTATGCCCGAGTTCTTTC 3′	
Rat eNOS	eNOS-2571-F	5′ CCAGGCTCTCACTTACTTC C 3′	151
NM_021838	eNOS-2721-R	5′ GAACCACTTCCATTCTTCGTA 3′	
Rat ET-1	ET1-348-F	5′ CTCCTGCTCCTCCTTGATGG 3′	169
NM_012548	ET1-516-R	5′ TCTGTTCCCTTGGTCTGTGG 3′	
Rat PAI-1	PAI-1-1983-F	5′ TTGCTCTTTATCCTGGGTCTC 3′	124
M24067.1	PAI-1-2106-R	5′ CTCCTTAATAGTGCTTCTTCTCC 3′	
Cyclophilin A (CPH)	CPH-96-F	5′-CTCCTTTGAGCTGTTTGCAG-3′	325
BC106030	CPH-420-R	5′-CACCACATGCTTGCCAT-3′	

Statistical analysis

Data calculation and statistical analysis were performed using the Stat View program (Abacus Concepts, Inc, Berkley, CA, USA). Data are presented as mean $\pm$ SD. Statistical differences between two groups were calculated by the unpaired Student's *t*-test. All data are distributed to ensure that the use of means and *t*-test is appropriate. A *P* value less than 0.05 denoted the presence of a statistically significant difference.

Results

Plasma adiponectin concentrations in Ad-Adipo rats

Ad-Adipo or Ad-lacZ was administered intravenously to diabetic male Wistar rats at 10 weeks after STZ injection. As shown in Figure 1a, administration of Ad-Adipo induced adiponectin expression in the liver, whereas no liver expression was detected in control rats given Ad-lacZ.

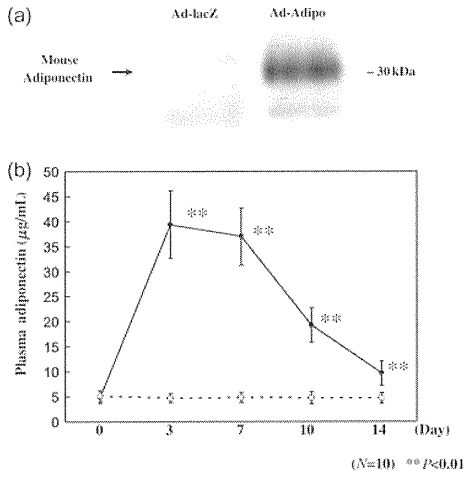

Figure 1 Adenoviral transduction of mouse adiponectin. (a) Liver extracts were immunoblotted with antiadiponectin antibody on day 14 after adenoviral administration. (b) Plasma adiponectin concentrations were measured from plasma samples obtained on day 0, 3, 7, 10 and 14, after administration in Ad-lacZ (□; $n = 10$) and Ad-Adipo (•; $n = 10$) using a mouse/rat adiponectin ELISA kit. Data are presented as means $\pm$ SD of the data obtained from the analysis of Adv-lacZ and Adv-Adipo rats. $n = 10$ per each group. $^{**}P < 0.01$

To confirm the duration of adiponectin protein expression, adiponectin concentrations were measured from plasma samples obtained at multiple points after adenovirus injection using a mouse/rat adiponectin ELISA kit. Figure 1b shows the time course of adiponectin content in the plasma of Ad-Adipo rats and Ad-lacZ rats (control group). Plasma concentrations increased fairly rapidly on day 3, were sustained until day 7 and declined gradually from days 7 to 14. We therefore conducted all subsequent *in vivo* experiments at two weeks after adenovirus administration, at which time, plasma adiponectin concentrations were within the physiological range (day 14 versus day 0).

Overall animal characteristics

STZ-injected rats exhibited severe hyperglycemia (>350 mg/dL) throughout the 12-week study period. They also displayed polydipsia and polyuria. Table 2 illustrates some of the general characteristics of the Ad-Adipo and control Ad-lacZ animals before and after two weeks adenovirus injection. Body weight and fasting glucose concentrations were similar between Ad-lacZ and Ad-Adipo diabetic rats before adenovirus injection. After two weeks adenovirus injection, body weight and fasting glucose were also similar between Ad-lacZ and Ad-Adipo diabetic rats (blood glucose 608.4 $\pm$ 42.9 versus 581.5 $\pm$ 26.9 mg/dL; body weight 443.6 $\pm$ 19.6 versus 437.6 $\pm$ 23.4 g). Moreover,

Table 2 Body weight and basal plasma measurements in the rats injected with Ad-Adipo versus control Ad-lacZ

	Ad-lacZ group (control) (*n*)	Ad-Adipo group (*n*)
Day 0		
Body weight (g)	410.2 $\pm$ 28.2 (10)	408.0 $\pm$ 25.4 (10)
Fasting plasma glucose (mg/dL)	610.2 $\pm$ 28.8 (10)	598.9 $\pm$ 23.4 (10)
Proteinuria (g/gCr)	0.83 $\pm$ 0.18 (10)	0.85 $\pm$ 0.21 (10)
Day 14 after adenovirus injection		
Body weight (g)	443.6 $\pm$ 19.6 (10)	437.6 $\pm$ 23.4 (10)
Fasting plasma glucose (mg/dL)	608.4 $\pm$ 42.9 (10)	581.5 $\pm$ 26.9 (10)
Fasting insulin (μU/mL)	0.38 $\pm$ 0.10 (10)	0.37 $\pm$ 0.17 (10)
Creatinine (mg/dL)	0.31 $\pm$ 0.03 (10)	0.30 $\pm$ 0.01 (10)

plasma creatinine concentrations were not different between the control and Ad-Adipo groups (0.31 ± 0.03 versus 0.30 ± 0.01 mg/dL).

Ad-Adipo rats exhibits decreased proteinuria

Proteinuria is considered to play a central role in the pathogenesis of progressive renal dysfunction. Therefore, we measured the degree of proteinuria by collecting the 24-h urine from each rat in individual metabolic cages. Before adenovirus injection, the degree of proteinuria was not significant difference with two groups (Table 2). After two weeks adenovirus injection, the degree of proteinuria was significantly reduced by 24.3%, from 1.63 ± 0.43 to 1.23 ± 0.49 g/d in Ad-Adipo rats compared with Ad-lacZ rats (Figure 2; $P < 0.05$), indicating an improvement of early diabetic nephropathy in hyperadiponectinemic animals.

Reduced TGF-β mRNA and protein expression levels in the renal cortex of Ad-Adipo animals

TGF-β1 contributes to the cellular hypertrophy and increased synthesis of collagen, both of which occur in diabetic nephropathy.[14,15] To elucidate the mechanism(s) whereby adiponectin could decrease proteinuria, we investigated whether adiponectin over-expression could alter profibrotic TGF-β expression in the renal cortex. We performed quantitative realtime reverse transcriptase (RT)-PCR on total RNA from the renal cortex of Ad-Adipo and Ad-lacZ rats. As shown in Figure 3a, TGF-β mRNA expression levels were significantly decreased by 31.7% in the renal cortex of Ad-Adipo rats when compared with that of Ad-lacZ rats ($P < 0.01$). Next, we evaluated TGF-β protein levels in the renal cortex of Ad-Adipo and Ad-lacZ rats. As shown in Figure 3b, TGF-β protein levels were significantly decreased by 50.1% in the renal cortex of Ad-Adipo rats when compared with that of Ad-lacZ rats ($P < 0.01$). Furthermore, representative photographs of immunohistochemical staining of TGF-β are presented in Figure 4. TGF-β proteins were decreased in the glomeruli of Ad-Adipo rats when compared with that of Ad-lacZ rats.

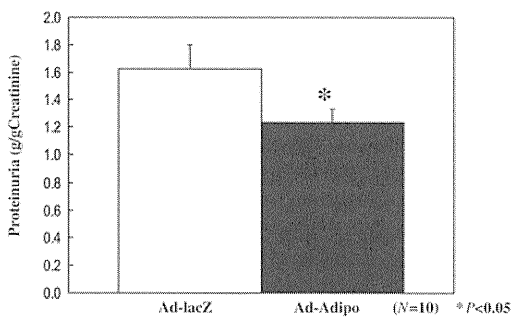

Figure 2 Proteinuria in streptozotocin (STZ)-induced diabetic rats on two weeks postinjection. At two weeks after lacZ (white bar) or Adipo (black bar) adenovirus administration to STZ-induced diabetic rats, total proteinuria was calculated by measuring urinary concentration of total protein and total urine volume. Data are presented as means $\pm$ SD of the data obtained from the analysis of Adv-lacZ and Adv-Adipo rats. $n = 10$ per each group. $^*P < 0.05$

Increased nephrin mRNA expression levels in the renal cortex of Ad-Adipo rats

Podocytes are important for the maintenance of the dynamic functional barrier.[3] Nephrin, a protein found in these cells, is crucial for maintaining the integrity of the intact filtration barrier and the renal expression of nephrin might be impaired in diabetic nephropathy.[5] We performed quantitative realtime RT-PCR on total RNA from the renal cortex of Ad-Adipo and Ad-lacZ rats to determine whether adiponectin over-expression impacts nephrin gene expression. As illustrated in Figure 3c, nephrin mRNA expression levels were significantly increased by 68.0% in the renal cortex of Ad-Adipo rats compared with that of Ad-lacZ rats ($P < 0.01$). These results suggested that adiponectin may reduce the degree of proteinuria via the downregulation of profibrotic TGF-β and upregulation of nephrin expression.

Improved endothelial function in the renal cortex of STZ-induced Ad-Adipo diabetic rats

Endothelial dysfunction correlates with progression of diabetic nephropathy. Therefore we determined levels of several markers of endothelial function in the renal cortex of Ad-Adipo and Ad-lacZ diabetic rats by quantitative realtime RT-PCR analysis. Proinflammatory endothelin 1 (ET-1) and plasminogen activator inhibitor 1 (PAI-1) mRNA expression levels were significantly decreased by 33.4% (Figure 5a; $P < 0.01$) and 34.7% (Figure 5b; $P < 0.01$) in the renal cortex of Ad-Adipo rats compared with Ad-lacZ rats, respectively. Endothelial nitric oxide synthase (eNOS) mRNA expression levels were significantly increased (117.2%, Figure 5c; $P < 0.01$) in the renal cortex of Ad-Adipo rats versus Ad-lacZ rats whereas inducible nitric oxide synthase (iNOS) mRNA expression levels were significantly decreased (40.3%, Figure 5d; $P < 0.05$). Together, these findings suggest that hyperadiponectinemia can reduce endothelial deterioration in diabetic nephropathy.

Discussion

Adiponectin is a recently described adipocyte-secreted polypeptide that can exert systemic effects on insulin sensitivity, lipid metabolism and inflammatory processes.[16] Circulating levels of adiponectin are decreased in a variety of insulin resistant states in man, including obesity and type 2 diabetes.[17] Adiponectin activity is most likely regulated at several levels, including gene expression, post-translational modification, oligomeric complex formation and receptor binding. To deliver ectopic expression of adiponectin *in vivo*, and to provide a physiologically relevant ligand capable of exerting systemic numerous effects of adiponectin, we developed an animal model of adiponectin over-expression using adenovirus-mediated gene transfer. The mouse adiponectin cDNA was cloned into an adenovirus vector, and the Ad-Adipo given to rats where it is targeted to the liver, with >90% of hepatocytes being infected as previously reported.[10] In turn, the liver cells secrete adiponectin

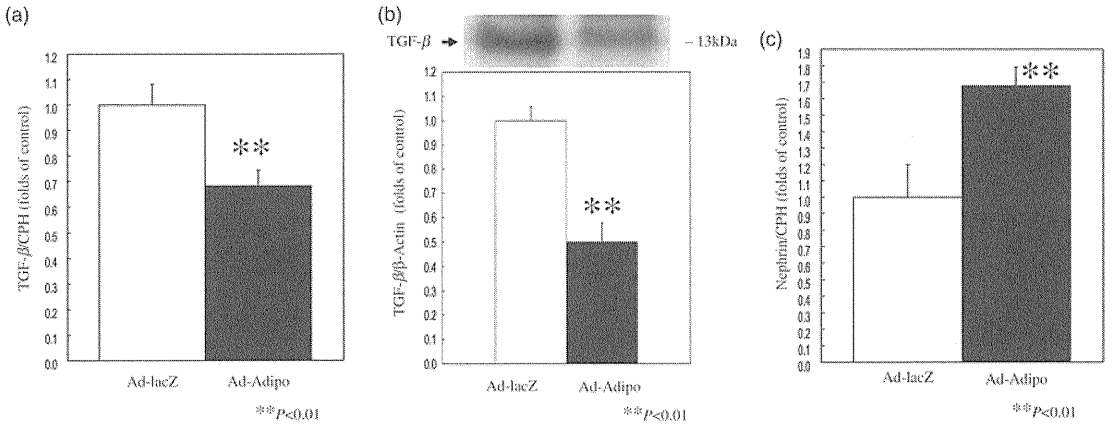

Figure 3 Effect of adiponectin on transforming growth factor β (TGF-β) and nephrin expression in the renal cortex tissue of streptozotocin (STZ)-induced diabetic rats. At two weeks after lacZ (white bar) or Adipo (black bar) adenovirus administration to STZ-induced diabetic rats, relative amounts of TGF-β (a) and nephrine (c) mRNA in the renal cortex tissue were determined by quantitative realtime polymerase chain reaction and corrected with cyclophilin A (CPH) as the internal standard ($n = 10$ in Ad-lacZ rats, $n = 10$ in Ad-Adipo rats). At two weeks after lacZ (white bar) or Adipo (black bar) adenovirus administration to STZ-induced diabetic rats, TGF-β (b) protein concentrations in the renal cortex tissue were determined by immunobloting analysis and corrected with β-actin as the internal standard ($n = 10$ in Ad-lacZ rats, $n = 10$ in Ad-Adipo rats). Data are presented as means $\pm$ SD of the data obtained from the analysis of Adv-lacZ and Adv-Adipo rats. $n = 10$ per each group. $^{**}P < 0.01$

into the circulation creating a chronic adiponectinemic state. In the present study, we examined the effects of physiological levels of adiponectin on diabetic nephropathy (Figure 1b).

We demonstrated that adiponectin reduced the degree of proteinuria in early diabetic nephropathy via the downregulation of TGF-β and upregulation of nephrin mRNA expression. We also showed that adiponectin overexpression led to improved intrarenal endothelial function in STZ-induced diabetic rats.

Proteinuria, the clinical manifestation of structural and functional defects in the glomerular filtration barrier, occurs often in the early stage of many forms of primary glomerular diseases, including diabetic nephropathy. A large body of evidence suggests that the podocyte foot processes and slit diaphragm are pivotal components of the glomerular filter, and disruption of their integrity is a critical event in the development of proteinuria and nephritic syndrome in a variety of inherited and acquired glomerular disorders.[18] Many genetic studies have underscored that podocyte slit diaphragm associated proteins, such as nephrin and podocin, play an essential role in establishing the size-selective filtration barrier of the kidney, and mutations or deletions of the genes encoding these proteins are consequently associated with the development of proteinuria in both animal models and patients.[19] Nephrin, a protein found in these cells, is crucial for maintaining the integrity of the intact filtration barrier. The renal expression of nephrin might be impaired in diabetic nephropathy as patients with diabetic nephropathy have markedly reduced renal nephrin expression and fewer electron-dense

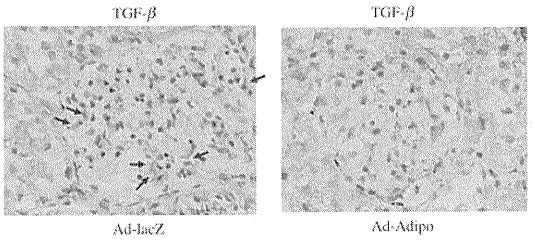

Figure 4 Effect of adiponectin on immunohistochemical staining with transforming growth factor β (TGF-β) and nephrin in the renal cortex tissue of streptozotocin (STZ)-induced diabetic rats. At two weeks after lacZ or Adipo adenovirus administration to STZ-induced diabetic rats, renal cortex tissue were harvested and processed. OCT compound-embedded sections were prepared for immunohistochemical staining with TGF-β antibody. Positive TGF-β staining was indicated by arrows. Original magnification: $\times$400 (A color version of this figure is appear in the online journal)

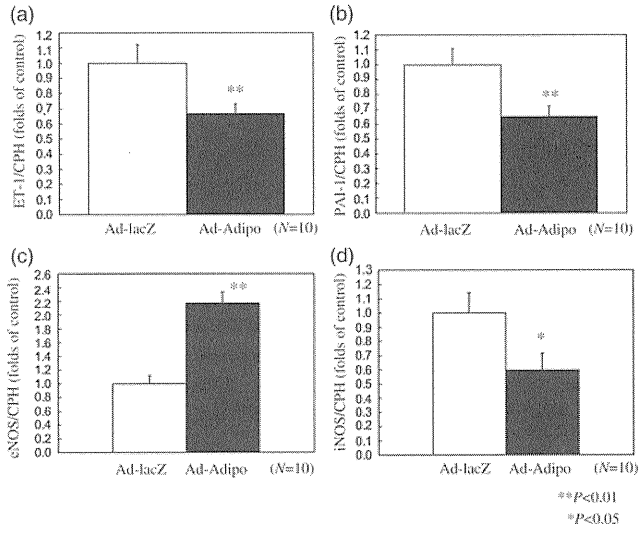

Figure 5 Effect of adiponectin on endothelin 1 (ET-1), plasminogen activator inhibitor 1 (PAI-1), endothelial nitric oxide synthase (eNOS) and inducible nitric oxide synthase (iNOS) mRNA in the renal cortex tissue of streptozotocin (STZ)-induced diabetic rats. At two weeks after lacZ (white bar) or Adipo (black bar) adenovirus administration to STZ-induced diabetic rats, relative amounts of ET-1 (a), PAI-1 (b), eNOS (c) and iNOS (d) mRNA in the renal cortex were determined by quantitative realtime polymerase chain reaction and corrected with cyclophilin A (CPH) as the internal standard ($n = 10$ in Ad-lacZ rats, $n = 10$ in Ad-Adipo rats). Data are presented as means $\pm$ SD of the data obtained from the analysis of Adv-lacZ and Adv-Adipo rats. $n = 10$ per each group. $^{*}P < 0.05$, $^{**}P < 0.01$

slit diaphragms compared with patients without diabetes and minimal nephropathic changes or controls.[5] Furthermore, nephrin excretion is raised 17–30% in patients with diabetes compared with individuals without diabetes. Thus, nephrin excretion could be an early finding of podocyte injury, even before the onset of albuminuria.[20] Hyperglycemia also increases the expression of TGF-β1 in the glomeruli and of matrix proteins specifically stimulated by this cytokine.[14] In the glomeruli of rats with STZ-induced diabetes, TGF-β1 concentrations are increased, and use of a neutralizing antibody to TGF-β1 prevents renal changes of diabetic nephropathy in these animals. In addition, connective tissue growth factor and heat shock proteins, which are encoded by TGF-β1-inducible genes, have fibrogenic effects on the kidneys of patients with diabetes. However, diabetes is associated with decreased expression of renal bone morphogenetic protein,[21] which in turn seems to counter the profibrogenic actions of TGF-β1.[14] Evidence clearly shows that TGF-β1 contributes to the cellular hypertrophy and increased synthesis of collagen, both of which occur in diabetic nephropathy.[14] Our findings are consistent with this current literature. We show that the renoprotective effects of adiponectin over-expression are associated with decreased TGF-β and increased nephrin gene expression.

In addition to glomerular abnormalities, endothelial dysfunction is another common feature in subjects with diabetic nephropathy.[22] It has been shown that diabetic subjects with renal disease often have an impaired release of nitric oxide (NO), and increased release of ET-1 and PAI-1.[23] We show that adiponectin can improve endothelial dysfunction by decreasing ET-1 and PAI-1 inflammatory gene expression. In addition, we found that adiponectin can also decrease iNOS and increase eNOS gene expression in the renal cortex as an alternate means to regulate endothelial function. These findings are in agreement with recent studies documenting that adiponectin can increase the phosphorylation of eNOS and NO production in endothelial cells[24] and inhibit the expression and proinflammatory activity of iNOS.[25]

We have shown that chronic hyperadiponectinemia inhibits the progression of glomerulo-endothelial dysfunction in early diabetic nephropathy. Adiponectin decreased the progression of proteinuria by decreasing TGF-β expression and increasing nephrin expression and improved endothelial dysfunction by decreasing ET-1, PAI-1 and iNOS gene expression while increasing eNOS gene expression in the renal cortex. Together, these results indicate that adiponectin treatment could serve as a therapy for diabetic nephropathy.

Author contributions: All authors contributed to the result interpretation and review of the manuscript. SN conducted the experiments and analysis of the data; AK and HH assisted the collection and analysis of quantitative RT-PCR data; YH performed the analysis of immunohistochemistry; SN and HS designed the experiments and wrote the manuscript; and TW contributed to manuscript preparation.

ACKNOWLEDGEMENTS

We are indebted to Yuko Ohashi and Atsuko Hashimoto for excellent technical assistance. This work was supported in part by a Fukushima Medical Foundation (HS), a Kanae Foundation for Life & Soci-Medical Science (HS), a Takeda Science Foundation (HS) and a Grant-in-Aid Scientific Research from the Ministry of Education, Culture, Sports, Science and Technology (HS).

REFERENCES

1 Remuzzi G, Schieppati A, Ruggenenti P. Clinical practice. Nephropathy in patients with type 2 diabetes. *N Engl J Med* 2002;**346**:1145–51
2 Ziyadeh FN. Mediators of diabetic renal disease: the case for tgf-beta as the major mediator. *J Am Soc Nephrol* 2004;**15** (Suppl. 1):S55–7
3 Mundel P, Shankland SJ. Podocyte biology and response to injury. *J Am Soc Nephrol* 2002;**13**:3005–15
4 Rhodes LA, Gustafson RA, Phillips JP, Cottrell L, Castillo W, Siu BL, Neal WA. The adult with congenital heart disease. *W V Med J* 2006;**102**:310–3
5 Benigni A, Gagliardini E, Tomasoni S, Abbate M, Ruggenenti P, Kalluri R, Remuzzi G. Selective impairment of gene expression and assembly of nephrin in human diabetic nephropathy. *Kidney Int* 2004;**65**:2193–200
6 Scherer PE, Williams S, Fogliano M, Baldini G, Lodish HF. A novel serum protein similar to C1q, produced exclusively in adipocytes. *J Biol Chem* 1995;**270**:26746–9
7 Maeda K, Okubo K, Shimomura I, Funahashi T, Matsuzawa Y, Matsubara K. cDNA cloning and expression of a novel adipose specific collagen-like factor, apM1 (AdiPose Most abundant Gene transcript 1). *Biochem Biophys Res Commun* 1996;**221**:286–9
8 Hu E, Liang P, Spiegelman BM. AdipoQ is a novel adipose-specific gene dysregulated in obesity. *J Biol Chem* 1996;**271**:10697–703
9 Nakano Y, Tobe T, Choi-Miura NH, Mazda T, Tomita M. Isolation and characterization of GBP28, a novel gelatin-binding protein purified from human plasma. *J Biochem (Tokyo)* 1996;**120**:803–12
10 Satoh H, Nguyen MT, Trujillo M, Imamura T, Usui I, Scherer PE, Olefsky JM. Adenovirus-mediated adiponectin expression augments skeletal muscle insulin sensitivity in male Wistar rats. *Diabetes* 2005;**54**:1304–13
11 Ouchi N, Kihara S, Arita Y, Okamoto Y, Maeda K, Kuriyama H, Hotta K, Nishida M, Takahashi M, Muraguchi M, Ohmoto Y, Nakamura T, Yamashita S, Funahashi T, Matsuzawa Y. Adiponectin, an adipocyte-derived plasma protein, inhibits endothelial NF-kappaB signaling through a cAMP-dependent pathway. *Circulation* 2000;**102**:1296–301
12 Becker B, Kronenberg F, Kielstein JT, Haller H, Morath C, Ritz E, Fliser D. Renal insulin resistance syndrome, adiponectin and cardiovascular events in patients with kidney disease: the mild and moderate kidney disease study. *J Am Soc Nephrol* 2005;**16**:1091–8
13 Sharma K, Ramachandrarao S, Qiu G, Usui HK, Zhu Y, Dunn SR, Ouedraogo R, Hough K, McCue P, Chan L, Falkner B, Goldstein BJ. Adiponectin regulates albuminuria and podocyte function in mice. *J Clin Invest* 2008;**118**:1645–56
14 Sharma K, Ziyadeh FN. Hyperglycemia and diabetic kidney disease. The case for transforming growth factor-beta as a key mediator. *Diabetes* 1995;**44**:1139–46
15 Benigni A, Zoja C, Corna D, Zatelli C, Conti S, Campana M, Gagliardini E, Rottoli D, Zanchi C, Abbate M, Ledbetter S, Remuzzi G. Add-on anti-TGF-beta antibody to ACE inhibitor arrests progressive diabetic nephropathy in the rat. *J Am Soc Nephrol* 2003;**14**:1816–24
16 Yamauchi T, Kamon J, Waki H, Terauchi Y, Kubota N, Hara K, Mori Y, Ide T, Murakami K, Tsuboyama-Kasaoka N, Ezaki O, Akanuma Y, Gavrilova O, Vinson C, Reitman ML, Kagechika H, Shudo K, Yoda M, Nakano Y, Tobe K, Nagai R, Kimura S, Tomita M, Froguel P, Kadowaki T. The fat-derived hormone adiponectin reverses insulin resistance associated with both lipoatrophy and obesity. *Nat Med* 2001;**7**:941–6
17 Yang WS, Lee WJ, Funahashi T, Tanaka S, Matsuzawa Y, Chao CL, Chen CL, Tai TY, Chuang LM. Weight reduction increases plasma levels of an adipose-derived anti-inflammatory protein, adiponectin. *J Clin Endocrinol Metab* 2001;**86**:3815–9
18 Pavenstadt H, Kriz W, Kretzler M. Cell biology of the glomerular podocyte. *Physiol Rev* 2003;**83**:253–307
19 Schwarz K, Simons M, Reiser J, Saleem MA, Faul C, Kriz W, Shaw AS, Holzman LB, Mundel P. Podocin, a raft-associated component of the

glomerular slit diaphragm, interacts with CD2AP and nephrin. *J Clin Invest* 2001;**108**:1621–9
20 Wolf G, Ziyadeh FN. Cellular and molecular mechanisms of proteinuria in diabetic nephropathy. *Nephron Physiol* 2007;**106**:p26–31
21 Steinke JM, Sinaiko AR, Kramer MS, Suissa S, Chavers BM, Mauer M. The early natural history of nephropathy in type 1 diabetes: III. Predictors of 5-year urinary albumin excretion rate patterns in initially normoalbuminuric patients. *Diabetes* 2005;**54**:2164–71
22 Chan WB, Chan NN, Lai CW, So WY, Lo MK, Lee KF, Chow CC, Metreweli C, Chan JC. Vascular defect beyond the endothelium in type II diabetic patients with overt nephropathy and moderate renal insufficiency. *Kidney Int* 2006;**70**:711–6
23 Kang DH, Nakagawa T, Feng L, Johnson RJ. Nitric oxide modulates vascular disease in the remnant kidney model. *Am J Pathol* 2002;**161**:239–48
24 Hattori Y, Nakano Y, Hattori S, Tomizawa A, Inukai K, Kasai K. High molecular weight adiponectin activates AMPK and suppresses cytokine-induced NF-kappaB activation in vascular endothelial cells. *FEBS Lett* 2008;**582**:1719–24
25 Cai XJ, Li CJ, Chen L, Rong YY, Zhang Y, Zhang M. A hypothesis: adiponectin mediates anti-atherosclerosis via adventitia-AMPK-iNOS pathway. *Med Hypotheses* 2008;**70**:1044–7

(Received July 21, 2010, Accepted February 22, 2011)

Life Sciences 88 (2011) 1055–1062

Contents lists available at ScienceDirect

Life Sciences

journal homepage: www.elsevier.com/locate/lifescie

Pioglitazone upregulates adiponectin receptor 2 in 3T3-L1 adipocytes

Akihiro Kudoh, Hiroaki Satoh *, Hiroyuki Hirai, Tsuyoshi Watanabe

Department of Nephrology, Hypertension, Diabetology, Endocrinology, and Metabolism, Fukushima Medical University, 1 Hikarigaoka, Fukushima City, Fukushima, 960-1295, Japan

ARTICLE INFO

Article history:
Received 28 September 2010
Accepted 24 March 2011

Keywords:
Pioglitazone
PPAR-γ
AdipoR2
AMPK

ABSTRACT

Aims: Pioglitazone, a full peroxisome proliferator-activated receptor (PPAR)-γ agonist, improves insulin sensitivity by increasing circulating adiponectin levels. However, the molecular mechanisms by which pioglitazone induces insulin sensitization are not fully understood. In this study, we investigated whether pioglitazone improves insulin resistance via upregulation of either 2 distinct receptors for adiponectin (AdipoR1 or AdipoR2) expression in 3T3-L1 adipocytes.

Main methods: Glucose uptake was evaluated by 2-[^{3}H] deoxy-glucose uptake assay in 3T3-L1 adipocytes with pioglitazone treatment. AdipoR1 and AdipoR2 mRNA expressions were analyzed by qRT–PCR.

Key findings: We first confirmed that pioglitazone significantly increased insulin-induced 2-deoxyglucose (2-DOG) uptake in 3T3-L1 adipocytes. Next, we investigated the mRNA expression and regulation of AdipoR1 and AdipoR2 after treatment with pioglitazone. Interestingly, pioglitazone significantly induced AdipoR2 expression but it did not affect AdipoR1 expression. In addition, adenovirus-mediated PPARγ expression significantly enhanced the effects of pioglitazone on insulin-stimulated 2-DOG uptake and AdipoR2 expression in 3T3-L1 adipocytes. These data suggest that pioglitazone enhances adiponectin's autocrine and paracrine actions in 3T3-L1 adipocytes via upregulation of PPARγ-mediated AdipoR2 expression. Furthermore, we found that pioglitazone significantly increased AMP-activated protein kinase (AMPK) phosphorylation in insulin-stimulated 3T3-L1 adipocytes, but it did not lead to the phosphorylation of IRS-1, Akt, or protein kinase Cλ/ζ.

Significance: Our results suggest that pioglitazone increases insulin sensitivity, at least partly, by PPARγ-AdipoR2-mediated AMPK phosphorylation in 3T3-L1 adipocytes. In conclusion, the upregulation of AdipoR2 expression may be one of the mechanisms by which pioglitazone improves insulin resistance in 3T3-L1 adipocytes.

Introduction

Insulin resistance is a primary defect underlying the development of type 2 diabetes mellitus and a central component defining the metabolic syndrome, a constellation of abnormalities that include obesity, hypertension, glucose intolerance, and dyslipidemia (Flier, 2004). Thiazolidinediones (TZDs) are pharmacologic agents that improve glucose homeostasis in type 2 diabetes by increasing insulin sensitivity, largely through improved insulin action in skeletal muscle (Olefsky, 2000). In addition, pioglitazone, which is one of the TZDs, significantly reduces the incidence of major adverse cardiovascular events, strokes, and all-cause mortality in high-risk patients with type 2 diabetes (Dormandy et al., 2005).

The antidiabetic actions of TZDs are believed to be mediated by their interaction with the nuclear receptor PPARγ (Lehmann et al., 1995). In both rodents and humans, adipose tissue is the main expression site for PPARγ, where in PPARγ is a key regulator of adipogenesis (Auboeuf et al., 1997). PPARγ is expressed at much lower levels in other tissues, including other major insulin target tissues, such as the skeletal muscle and liver (Spiegelman, 1998). The distribution of PPARγ expression suggests that the adipose tissue may be the primary target for the insulin-sensitizing effect of PPARγ agonists such that changes in adipose tissue activity lead to improved insulin sensitivity in other tissues (Spiegelman, 1998). Indeed, TZDs markedly change gene expression in adipose tissue, yielding smaller adipocytes whose altered secretion of adipocytokines may improve insulin resistance in other tissues (Okuno et al., 1998). Furthermore, TZDs are well known to cause an elevation of adiponectin levels in vivo and in vitro (Hirose et al., 2002).

Adiponectin (Hu et al., 1996; Maeda et al., 1996; Nakano et al., 1996; Scherer et al., 1995) is a hormone secreted by adipocytes, which function as the key antidiabetic and antiatherogenic adipocytokine (Scherer, 2006). Plasma adiponectin levels are decreased in obesity, insulin resistance, and type 2 diabetes mellitus (Scherer, 2006). Many studies have shown that the high levels of adiponectin are associated with insulin sensitization, whereas low levels are found in insulin resistance (Berg et al., 2001; Fruebis et al., 2001; Hotta et al., 2001; Satoh et al., 2005; Yamauchi et al., 2001). This insulin-sensitizing effect of adiponectin appears to be mediated by the inhibition of gluconeogenesis (Berg et al., 2001) and the stimulation of fatty acid oxidation (Fruebis et al., 2001; Yamauchi et al., 2001) via the activation of AMPK (Yamauchi et al., 2002).

* Corresponding author. Tel.: +81 24 547 1206; fax: +81 24 548 3044.
E-mail address: hiroakis-tky@umin.ac.jp (H. Satoh).

0024-3205/$ – see front matter © 2011 Elsevier Inc. All rights reserved.
doi:10.1016/j.lfs.2011.04.001

Recently, 2 distinct receptors for adiponectin (AdipoR1 and AdipoR2) have been identified (Yamauchi et al., 2003). In mice, AdipoR1 is abundantly expressed in the skeletal muscle, whereas AdipoR2 is predominantly expressed in the liver (Yamauchi et al., 2003). To elicit its cellular actions, adiponectin binds to AdipoR1 and AdipoR2 cell surface receptors, triggering signaling cascades that culminate in improved insulin action and/or sensitivity. Adiponectin receptors mediate the activation of AMPK, PPARα, and fatty acid oxidation, which increases glucose uptake and improves lipid metabolism (Yamauchi et al., 2003; Yamauchi et al., 2002). AMPK is a fuel-sensing enzyme that has been implicated in the regulation of glucose and lipid homeostasis and insulin sensitivity (Fisher et al., 2002). Activation of AMPK increases the insulin sensitivity of the muscle glucose transport involved in a step beyond the Akt/protein kinase B (PKB) pathway (Salt et al., 2000). However, the molecular mechanisms by which pioglitazone induces insulin sensitization are not fully understood.

In this study, we investigated whether pioglitazone improves insulin resistance via upregulation of either AdipoR1 or AdipoR2 expression in 3T3-L1 adipocytes.

Materials and methods

Materials

Pioglitazone was donated by Takeda Co (Tokyo, Japan). 3T3-L1 preadipocytes were purchased from American Type Cell Collection (Manassas, VA, USA). pAxCAwt plasmid vector was obtained from TAKARA Biomedical (Shiga, Japan). DMEM, streptomycin, trypsin, fetal bovine serum (FBS), TRIzol reagent, pCR2.1-TOPO vector, LDS sample buffer, and Sample Reducing Agent were from Invitrogen Life Technologies (Carlsbad, CA, USA). The RNeasy kit was obtained from QIAGEN Inc. (Valencia, CA, USA). Anti-phospho-specific Akt (Ser473 and Thr308), anti-Akt, anti-phospho-specific AMPK (Thr172), anti-AMPK, anti-phospho-specific-PKCλ/ζ (Thr410/403) and anti-β-actin antibodies were from Cell Signaling Technology (Boston, MA, USA). Anti-insulin receptor substrate (IRS)-1 (Tyr508) antibody was obtained from Millipore Corp (Billerica, MA, USA). PPARγ siRNA (sc29455), Anti-IRS-1, Anti-PPARγ1, and horseradish peroxidase-conjugated secondary antibodies were from Santa Cruz Biotechnology (Santa Cruz, CA, USA). Polyvinylidine difluoride (PVDF) transfer membranes were purchased from Millipore Corp. (Bedford, MA, USA). iScript cDNA Synthesis Kit and iQ SYBR Green Supermix were from Bio-Rad Laboratories (Richmond, CA, USA). 2-[^{3}H] Deoxyglucose was purchased from PerkinElmer Inc. (Waltham, MA, USA).

Subcloning of the mouse PPARγ1 cDNA by RT–PCR

The mouse full-length PPARγ1 cDNA (1428 bp) was amplified from mouse liver using 5′-CCATGGTTGACACAGAGATGCCATTC-3′ sense, and 5′-GGGTGGGACTTTCCTGCTAATAC-3′ antisense primers, and subcloned into the pCR2.1-TOPO and sequenced, confirming that the clones corresponded to the mouse PPARγ1 (GenBank accession number U01841).

Construction of recombinant adenoviruses

PPARγ1 adenovirus (Ad-PPARγ1) and lacZ adenovirus (Ad-lacZ) were generated and purified using a previously described protocol (Satoh et al., 2004). Briefly, the mouse PPARγ1 cDNA was inserted in the pAxCAwt plasmid to generate pAxCAwt-mouse PPARγ1. The resulting plasmid, which contains the PPARγ1 cDNA under the control of a CAG promoter (CMV enhancer, chicken β-actin promoter, and part of an untranslated region of rabbit β-globin), was transfected into 293 cells. Recombinant Ad from a single plaque was expanded and purified twice by cesium chloride gradient ultracentrifugation. Viral titer was determined by plaque assay. Control Ad-lacZ that carries the β-galactosidase cDNA was isolated using the same procedure. Both recombinant viruses were dialyzed in PBS, pH 7.4, and stored in 10% glycerol/PBS at −80 °C until use.

Cell culture and cell treatment

3T3-L1 cells were cultured and differentiated as described previously (Nguyen et al., 2005). Differentiated 3T3-L1 adipocytes were incubated with the indicated concentration of pioglitazone, or 0.1% dimethyl sulfoxide vehicle for 3 or 6 h before each assay. For adenovirus infection, 3T3-L1 adipocytes were transduced for 2 h in DMEM high glucose with 2% heat-inactivated serum with the following multiplicity of infection (m.o.i.) and with either the recombinant adenovirus of PPARγ1 (40 m.o.i.) or control recombinant adenovirus of lacZ. The total amount of adenovirus was adjusted to the same m.o.i. as the control adenovirus in each experiment. On the other hand, for PPARγ knockdown experiments, 3T3-L1 adipocytes were transfected with optimized concentrations of either human PPARγ small interfering RNA (siRNA) (Cat. # sc-29455), control nonsense fluorescein conjugate siRNA (Cat. # sc-36869) using siRNA transfection reagent alone according to the manufacturer's instructions (Santa Cruz Biotechnology, Inc). Transduced cells were incubated for 48 h at 37 °C in 10% CO_2 and Dulbecco's modified Eagle's high glucose medium with 10% heat-inactivated serum, followed by incubation in the starvation media required for the assays.

2-Deoxyglucose uptake assay

Glucose uptake was initiated as described previously (Nguyen et al., 2005), with some modifications. After 48 h of adenovirus infection, 3T3-L1 adipocytes were serum-starved for 6 h, and the cells were stimulated with 100 ng/ml insulin in KRP-Hepes buffer (10 mM Hepes, pH7.4, 131.2 mM NaCl, 4.7 mM KCl, 1.2 mM $MgSO_4$, 2.5 mM $CaCl_2$, and 2.5 mM NaH_2PO_4) for 30 min at 37 °C. Glucose uptake was determined in triplicate at each point at the addition of 2-[^{3}H] deoxyglucose (0.1 μCi, final concentration 0.1 mM) in KRP-Hepes buffer for 5 min at 37 °C. The cells were washed in ice-cold PBS 3 times and solubilized in 1N NAOH. Each sample was subjected to liquid scintillation counting (Nguyen et al., 2005).

Quantitative real-time RT–PCR analysis

Total RNA samples were extracted from cells with TRIzol reagent, and total RNA was further purified using the RNeasy kit with RNase-free DNase I treatment according to the manufacturer's instructions. Total RNA (1 μg) was reverse-transcribed with iScript cDNA Synthesis Kit according to the manufacturer's instructions (Bio-Rad Laboratories, Inc). Quantitative real-time PCR was performed with a Bio-Rad system using iQ SYBR Green Supermix and specific primer pairs (Table 1) selected with Primer Express software (Applied Biosystems). The relative mass of specific RNAs was calculated by the comparative cycle of threshold detection method according to the manufacturer's instructions.

Table 1
Primers used for real-time RT–PCR.

	Forward	Reverse
mACRP30	5′-GCAACTACCCATAGCCCATAC-3′	5′-GCAACTACCCATAGCCCATAC-3′
mAdipoR1	5′-AGATGGAGGAGTTCGTGTATAAG-3′	5′-ATGTAGCAGGTAGTCGTTGTC-3′
mAdipoR2	5′-CCACAACCTTGCTTCATCTACC-3′	5′-ACGAACACTCCTGCTCTGAC-3′
CPH	5′-CACCACATGCTTGCCATCC-3′	5′-CTCCTTTGAGCTGTTTGCAG-3′

Immunoblotting analysis

Serum-starved 3T3-L1 cells were stimulated with 100 ng/ml insulin at 37 °C for various times as indicated in each experiment. The cells were lysed in solubilizing buffer containing 20 mM Tris, 1 mM EDTA, 140 mM NaCl, 1% Nonidet P-40 (NP-40), 50 U of aprotinin/ml, 1 mM Na_3VO_4, 1 mM PMSF, and 10 mM NaF (pH 7.5) for 30 min at 4 °C. The cell lysates were centrifuged at 15,000 rpm for 30 min at 4 °C, to remove insoluble materials. For western blot analysis, whole-cell lysates (10 μg protein per lane) were denatured by boiling in lithium dodecyl sulfate (LDS) sample buffer and Sample Reducing Agent (Invitrogen Life Technologies). Gels were transferred to PVDF membrane (Immobilon-P), using semi-dry Transblot apparatus (Bio-Rad Laboratories Inc.). For immunoblotting, membranes were blocked and probed with specified antibodies. Membranes were then incubated with horseradish peroxidase-conjugated secondary antibodies before chemiluminescence detection, according to the manufacturer's instructions (Pierce, Rockford, IL, USA). Band intensities were quantified by densitometry using the Image J software (NIH, USA).

Statistical analysis

Statistical analysis were performed using Excel statistics 2008 (SSRI, Tokyo, Japan) added in Excel software (Microsoft Corporation, USA). The data were analyzed by one-way ANOVA or unpaired two-tailed Student *t* test. A P-value of less than 0.05 was considered to indicate significance. All values are expressed as the means ± SE.

Results

Effects of pioglitazone on insulin-stimulated glucose transport at dose- and time-dependent manner in 3T3-L1 adipocytes

We first examined the effects of pioglitazone treatment for 6 h on insulin-stimulated glucose uptake in 3T3-L1 adipocytes. As shown in Fig. 1A, pretreatment of cells with pioglitazone led to a 35–65% increase ($P<0.01$) in insulin (100 ng/ml)-stimulated 2-deoxyglucose (2-DOG) uptake at concentrations of 0.5, 1, 2, 10, and 20 μM pioglitazone, respectively, whereas pioglitazone pretreatment did not induce any change in basal 2-DOG uptake. Pioglitazone significantly increased insulin-stimulated 2-DOG uptake within the range 0.5–2 μM in a dose-dependent manner. As shown in Fig. 1B, pretreatment of cells treated with 2 μM pioglitazone for 6 h resulted to a 50% increase ($P<0.01$) in insulin-stimulated 2-DOG uptake as compared with basal insulin-stimulated cells, whereas pretreatment with pioglitazone for 3 h did not significantly increase insulin-stimulated 2-DOG uptake. Ten μM pioglitazone also represented similar results (data not shown).

Effects of pioglitazone on the expression of adiponectin, AdipoR1, and AdipoR2 in 3T3-L1 adipocytes

Because the distribution of AdipoR1 and AdipoR2 expression varies between target tissues and among animal species, we hypothesized that adiponectin receptor distribution and/or upregulation by pioglitazone could play a role in enhancing insulin sensitivity in 3T3-L1 adipocytes. Next, we investigated whether treatment with pioglitazone could alter the expression of AdipoR1 and/or AdipoR2 in 3T3-L1 adipocytes. We performed quantitative real-time RT–PCR on total RNA from serum-starved 3T3-L1 adipocytes that were treated with or without pioglitazone (2 μM) for 3 h. As shown in Fig. 2, we confirmed that pioglitazone significantly increased adiponectin expression by 50% ($P<0.01$). Furthermore, pioglitazone significantly induced the expression of AdipoR2 by up to 2.5 fold ($P<0.01$), but it did not affect AdipoR1 expression.

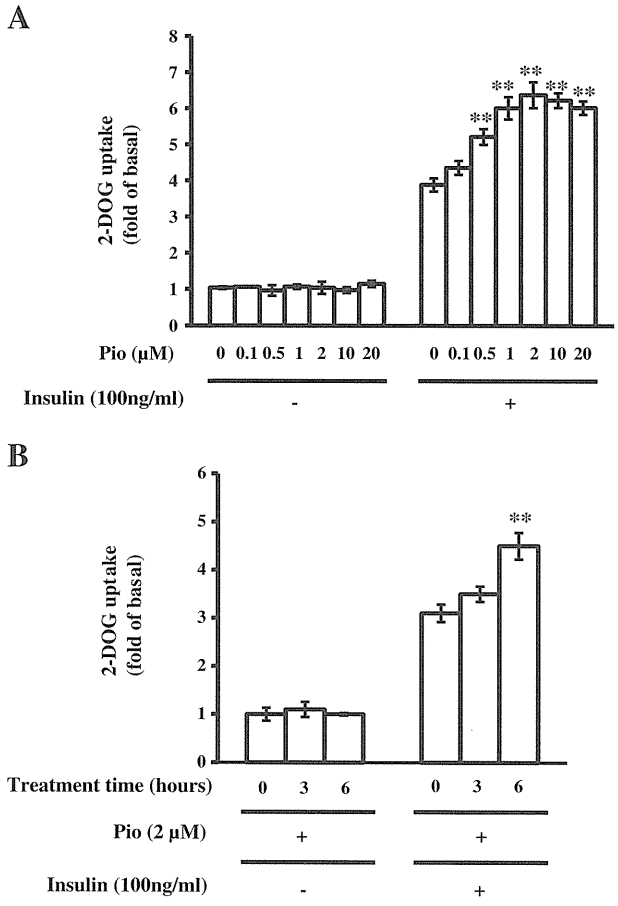

Fig. 1. Effects of pioglitazone on insulin-stimulated 2-DOG uptake in 3T3-L1 adipocytes. (A) After pretreatment without or with pioglitazone (Pio) (0.1, 0.5, 1.0, 2, 10, and 20 μM) for 6 h, serum-starved 3T3-L1 adipocytes were treated with insulin (100 ng/ml) for 30 min, followed by measurement of 2-DOG uptake. (B) After pretreatment without or with pioglitazone (2 μM) for 0, 3, or 6 h, serum-starved 3T3-L1 adipocytes were treated with insulin (100 ng/ml), followed by measurement of 2-DOG uptake. Data represent the mean ± SE of 3 independent experiments (1 experiment performed with 3 samples). $^{**}P<0.01$.

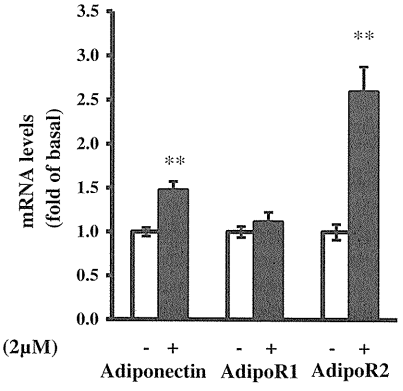

Fig. 2. Effects of pioglitazone on the expression mRNA of adiponectin, AdipoR1, and AdipoR2 in 3T3-L1 adipocytes. Serum-starved 3T3-L1 adipocytes were treated without or with pioglitazone (2 μM) for 3 h. Total RNA extracted from all cells was used for gene expression analysis of adiponectin, AdipoR1, and AdipoR2. Levels of CPH were used for normalization of sample loading. Data represent the mean ± SE of 3 independent experiments (1 experiment performed with 6 samples). $^{**}P<0.01$.

PPARγ enhanced the effect of pioglitazone in 3T3-L1 adipocytes

Pioglitazone is a ligand for the high level of PPARγ1 protein expression in 3T3-L1 adipocytes and HEK293 cells; therefore, we performed western blotting of cell lysates obtained from either Ad-PPARγ1- or Ad-lacZ-infected cells. The expression of PPARγ1 protein in Ad-PPARγ1-infected 3T3-L1 adipocytes was higher by 1.5 fold ($P<0.01$) as compared to that in Ad-lacZ-infected controls (Fig. 3A and B). We next examined 2-DOG uptake in Ad-PPARγ1- or Ad-lacZ-infected 3T3-L1 adipocytes. PPARγ1 overexpressed cells without pioglitazone pretreatment did not exhibit increase in insulin-stimulated 2-DOG uptake as compared to control cells without pioglitazone pretreatment. In contrast, PPARγ1 overexpressed cells with 10 μM pioglitazone pretreatment for 6 h exhibited an ~16% increase ($P<0.05$) in insulin-stimulated 2-DOG uptake as compared to control cells with pioglitazone pretreatment (Fig. 4). These results suggest that these effects of pioglitazone may be regulated by the amount of PPARγ protein expression in 3T3-L1 adipocytes.

To further assess whether PPARγ1 overexpression alters adiponectin, AdipoR1, and/or AdipoR2 expression, we performed quantitative real-time RT–PCR on the total RNA from PPARγ overexpressed 3T3-L1 adipocytes and that obtained from control cells. As shown in Fig. 5, adiponectin expression was significantly enhanced (11%; $P<0.05$) in PPARγ1 overexpressed cells as compared to that in control cells. Furthermore, AdipoR2 expression was significantly enhanced (34%; $P<0.01$) in PPARγ1 overexpressed cells as compared to that in control cells, whereas AdipoR1 expression was not enhanced in PPARγ1 overexpressed cells.

PPARγ-konckdown diminished the pioglitazone-induced AdipoR2 expression in 3T3-L1 adipocytes

Whether PPARγ-knockdown alters AdipoR1 or/and AdipoR2 expression, we performed quantitative real-time RT–PCR on the total RNA from PPARγ-specific siRNA transfected 3T3-L1 adipocytes. As shown in Fig. 6, AdipoR2 expression was reduced in PPARγ-specific siRNA transfected cells compared with the control cells with pioglitazone treatment conditions, whereas AdipoR1 expression was not changed between PPARγ-specific siRNA transfected cells and control cells.

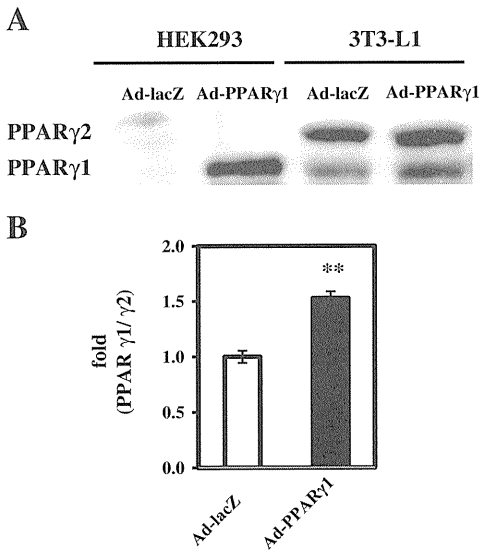

Fig. 3. Analysis of adenovirus infected 3T3-L1 adipocytes and HEK293 cells for mouse PPARγ1 expression. 3T3-L1 adipocytes and HEK293 cells were transduced with Ad-PPARγ1 or Ad-lacZ (control). At 48 h after infection, cell lysates were prepared as described in the Materials and methods section. Whole-cell lysates (10 μg) were subjected to LDS-PAGE and transferred to PVDF membrane, and PPARγ1 was detected using a polyclonal Ab against mouse PPARγ. Data represent the mean ± SE of 4 independent experiments. $^{**}P<0.01$.

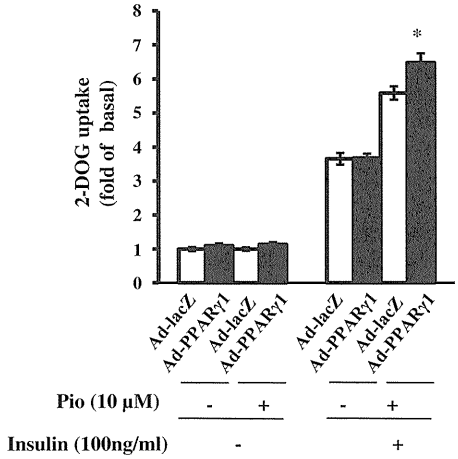

Fig. 4. Effects of PPARγ1 over-expression on 2-DOG uptake in 3T3-L1 adipocytes. 3T3-L1 adipocytes were transduced with Ad-PPARγ1 or Ad-lacZ for 48 h, and after pretreatment with or without pioglitazone (10 μM) for 6 h, serum-starved 3T3-L1 adipocytes were treated with insulin (100 ng/ml), followed by measurement of 2-DOG uptake. Data represent the mean ± SE of 3 independent experiments (1 experiment performed with 3 samples). $^{*}P<0.05$.

Effects of pioglitazone treatment on insulin-stimulated IRS-1, Akt, PKCλ/ξ, and AMPK phosphorylation in 3T3-L1 adipocytes

The serine/threonine kinase Akt and threonine kinase PKCλ/ξ are the key molecules in the insulin signaling pathway (Saltiel and Kahn, 2001). To assess the potential cellular mechanisms by which the pioglitazone induces increase in insulin sensitivity, we first determined whether pioglitazone affects the activation of insulin-signaling key components by measuring insulin-stimulated Akt and PKCλ/ξ protein levels and phosphorylation. We pretreated 3T3-L1 adipocytes with pioglitazone

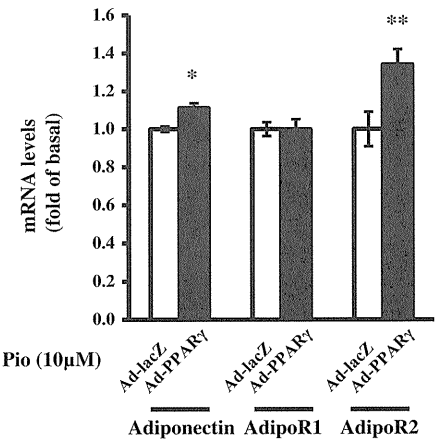

Fig. 5. Effects of pioglitazone on expression of adiponectin, AdipoR1, and AdipoR2 in PPARγ1 over-expressed 3T3-L1 adipocytes. 3T3-L1 adipocytes were transduced with Ad-PPARγ1 or Ad-lacZ. At 48 h after infection, serum-starved 3T3-L1 adipocytes were treated without or with pioglitazone (10 μM) for 3 h. Total RNA extracted from all cells was used for gene expression analysis of adiponectin, AdipoR1, and AdipoR2. Levels of CPH were used for normalization of sample loading. Data represent the mean ± SE of 3 independent experiments (1 experiment performed with 6 samples). $^{**}P<0.01$.

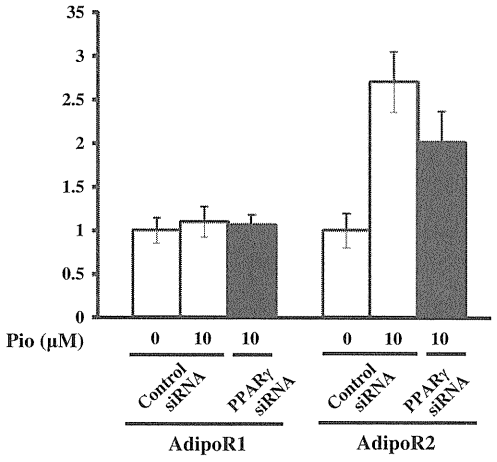

Fig. 6. Effects of pioglitazone on expression of AdipoR1 and AdipoR2 in PPARγ knock-downed 3T3-L1 adipocytes. 3T3-L1 adipocytes were transduced with PPARγ -siRNA. At 48 h after induction, serum-starved 3T3-L1 adipocytes were treated without or with pioglitazone (10 μM) for 3 h. Total RNA extracted from all cells was used for gene expression analysis of AdipoR1, and AdipoR2. Levels of CPH were used for normalization of sample loading. Data represent the mean ± SE of 3 independent experiments.

for 6 h, and subsequently stimulated the cells with insulin. Cell lysates were then analyzed by LDS-PAGE, followed by western blotting with antibodies against IRS-1 (phospho-specific IRS-1 antibodies directed against Tyr508), Akt (phospho-specific Akt antibodies directed against Ser437 or Thr308), PKCλ/ξ (phospho-specific PKCλ/ξ antibodies directed against Thr410/Thr403). In the absence of insulin stimulation, pioglitazone did not induce any change in phospho-Akt (Thr308 or Ser437), phospho-PKCλ/ξ, and AMPK phosphorylation (Thr172). Further, 10 min of insulin stimulation led to an increase in Akt and PKCλ/ξ activation, as assessed by the phospho-Akt antibodies (Thr308 or Ser437), without changing the protein levels. Pretreatment of cells with pioglitazone for 6 h did not alter Akt protein levels, Akt phosphorylation (Ser437 and Thr308), and PKCλ/ξ phosphorylation (Thr410/403) after insulin treatment (Fig. 7A–D). These results suggest that pioglitazone increases insulin sensitivity via a pathway that is independent of both Akt- and PKCλ/ξ-mediated signaling cascade pathways in the acute phase.

We also assessed AMPK, which is a key molecule in the AdipoR-mediated signaling pathway (Yamauchi et al., 2003), by measuring insulin-stimulated AMPK protein levels and phosphorylation. AMPK phosphorylation (Thr172) was significantly increased (70%; $P<0.01$) in the cells that were pretreated with pioglitazone for 6 h as compared

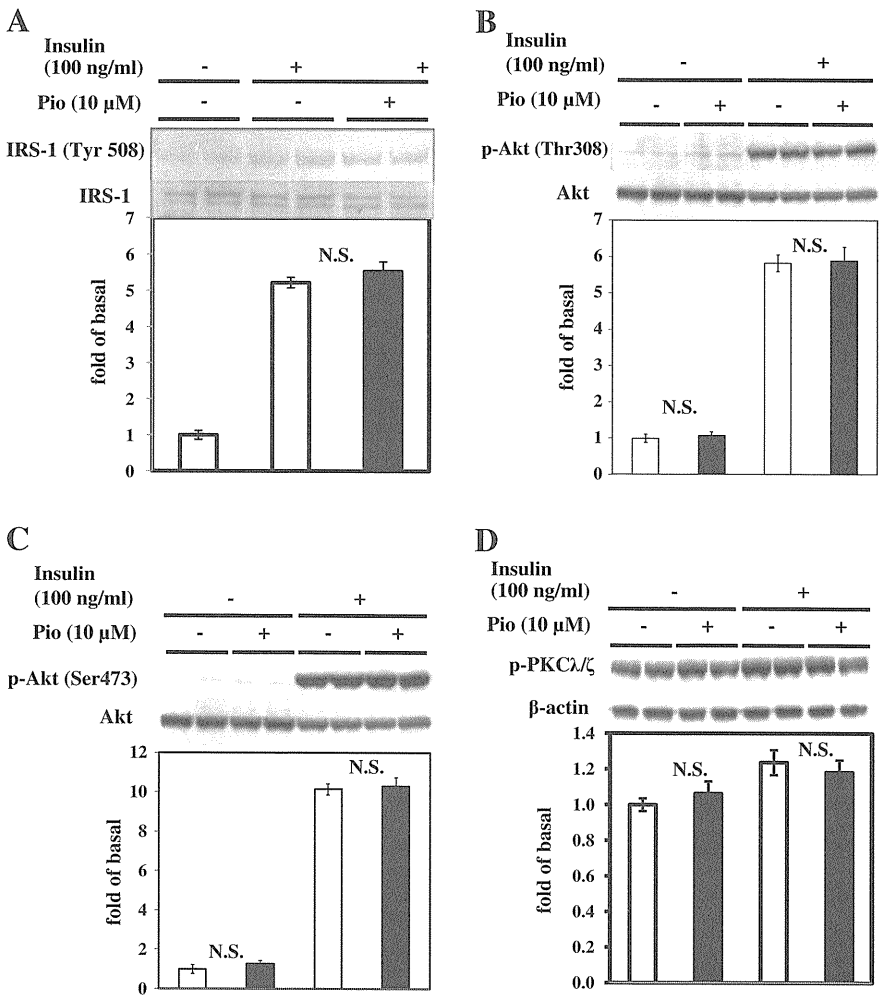

Fig. 7. Effect of pioglitazone on intracellular insulin signaling such as IRS-1, Akt, and PKCλ/ζ. Serum-starved 3T3-L1 adipocytes were pretreated with or without pioglitazone (10 μM) for 6 h and stimulated with insulin (100 ng/ml) for 10 min. Cell lysates were prepared as described in the Materials and methods section. Whole-cell lysates (10 μg) were subjected to LDS-PAGE and immunoblotted with anti-IRS-1 (Tyr508) (A), anti-phospho-specific Akt (pAKT) threonine 308 (B) and serine 437 (C), anti-Akt-1, and anti-phospho-specific-PKCλ/ζ (Thr410/403) (D). Data represent the mean ± SE of 3 independent experiments (1 experiment performed with 2 samples). $^{**}P<0.01$.

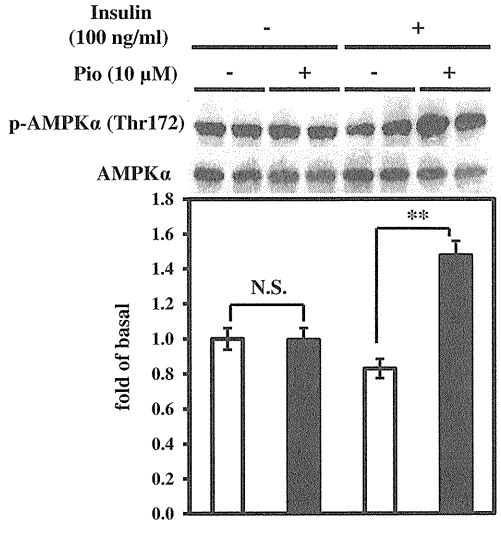

Fig. 8. Effect of pioglitazone on intracellular signaling about AMPK. Serum-starved 3T3-L1 adipocytes were pretreated with or without pioglitazone (10 μM) for 6 h and stimulated with insulin (100 ng/ml) for 10 min. Cell lysates were prepared as described in the Materials and methods section. Whole-cell lysates (10 μg) were subjected to LDS-PAGE and immunoblotted with anti-phospho-specific AMPKα (Thr172) and anti-AMPKα antibodies.

to that in insulin-stimulated cells without pioglitazone, whereas the total AMPK protein content remained unchanged (Fig. 8).

Discussion

Pioglitazone is an antidiabetic insulin-sensitizing agent that improves insulin action in a variety of animal states of insulin resistance and diabetes (Olefsky, 2000). Although it is known that pioglitazone functions as a ligand for PPARγ, the molecular mechanisms underlying its insulin-sensitizing effects are not well understood. As shown in Fig. 9, we showed that pioglitazone upregulates PPARγ1-mediated AdipoR2 expression in the acute phase in 3T3-L1 adipocytes. These findings raised the possibility results that pioglitazone may enhance adiponectin's autocrine and paracrine action via the upregulation of AdipoR2 expression in insulin treated 3T3L1 adipocytes.

AdipoR1 and AdipoR2, 2 distinct receptors for adiponectin, have been cloned (Yamauchi et al., 2003). Many studies have shown that both AdipoR1 and AdipoR2 play a crucial role in glucose and lipid metabolism (Caminos et al., 2005; Tan et al., 2005; Tsuchida et al., 2004; Vaxillaire et al., 2006; Yamauchi et al., 2007). The expressions of both AdipoR1 and AdipoR2 were significantly decreased in the muscle and adipose tissue in obese mice (Tsuchida et al., 2004). The disruption of both AdipoR1 and AdipoR2 in the mouse liver abolished adiponectin binding and actions, resulting in increased tissue triglyceride content, inflammation, and oxidative stress, thereby leading to insulin resistance and marked glucose intolerance (Yamauchi et al., 2007). Conversely, adenovirus-mediated overexpressions of AdipoR1 or AdipoR2 in the liver of obese mice enhanced the effects of adiponectin such as the activation of AMPK and PPARα in the liver.

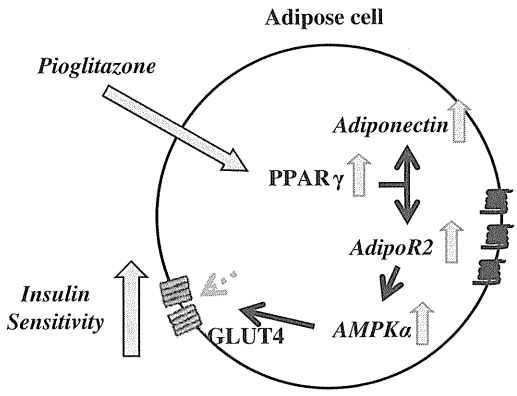

Fig. 9. Schematic of the hypothetical mechanisms of improvement in insulin sensitivity by pioglitazone in 3T3-L1 adipocytes. Pioglitazone increases insulin sensitivity via AdipoR2-mediated AMP-activated protein kinase phosphorylation in 3T3-L1 adipocytes.

A central finding in our study is that pioglitazone enhances insulin sensitivity, as manifested by an upregulation of AdipoR2 and adiponectin in 3T3-L1 adipocytes. This observation is consistent with two previous reports that have demonstrated positive effects of pioglitazone on adiponectin receptor expression (Coletta et al., 2009; Shimizu et al., 2007). Thus, Shimizu et al. have reported that pioglitazone upregulates AdipoR2 mRNA and protein in a hepatocyte cell line (Shimizu et al., 2007). And Coletta et al. have also reported that pioglitazone upregulates AdipoR1 and AdipoR2 mRNA in the human skeletal muscle (Coletta et al., 2009). In contrast, Li et al. (Li et al., 2007) had previously showed that both adiponectin receptors are expressed in cellular fractions of human adipocytes, but TZD administration did not affect expression of either AdipoR1 or AdipoR2, while improving insulin action and increasing adiponectin levels. This contrasts with the finding in the current study and previous reports (Coletta et al., 2009; Shimizu et al., 2007). Although we do not know the precise mechanism underlying these differences in experimental results, one possibility exists, one of which likely arises from differential designs. The results in the human study (Li et al., 2007) were conducted in hyperinsulinemic euglycemic clamp study for 6 h. It has been reported that both AdipoR1 and AdipoR2 expressions are reduced by the long-term stimulation of insulin (Tsuchida et al., 2004). In contrast, we evaluated the pioglitazone induced AdipoR2 expression in condition with short-term insulin stimulation. Thus it is possible that, the long term-treatment of insulin may attenuate the pioglitazone induced AdipoR2 expression.

Furthermore, human genetic analysis has shown a contribution of AdipoR2 variants in diabetes risk in the French population (Vaxillaire et al., 2006). Therefore, a therapeutic strategy would be to upregulate adiponectin receptors. We showed that pioglitazone augments the expression of AdipoR2 in adipocytes. Further, PPARα agonists also regulate the expression of adiponectin receptors in adipocytes and macrophages (Tsuchida et al., 2005).

Two PPAR isoforms, PPARγ1 and PPARγ2, are expressed in ubiquitous tissues, although PPARγ2 is much less abundant than PPARγ1 (Sakamoto et al., 2000). We first confirmed the adenovirus-mediated overexpression of PPARγ1 (Ad-PPARγ1) in 3T3-L1 adipocytes (Fig. 3). In PPARγ1 overexpressed cells, pioglitazone increased insulin-stimulated 2-DOG uptake as compared to that in control cells with pioglitazone pretreatment (Fig. 5). This effect disappeared in the absence of pioglitazone. It has been known that as endogenous PPARγ ligands, some fatty acid and lipid mediators in the arachidonate cascade play a crucial role during adipocyte differentiation (Tzameli et al., 2004). Our results suggest that endogenous ligands may not lead to increased glucose uptake in the PPARγ1 overexpressed 3T3-L1 adipocytes. Pioglitazone increased adiponectin expression in addition to AdipoR2 expression in PPARγ1 overexpressed cells (Fig. 5). The data obtained in this study suggest a potential explanation for the pioglitazone-induced increase in insulin-stimulated glucose uptake. Furthermore, these data suggest that AdipoR2 may be targeted by PPARγ1 in 3T3-L1 adipocytes.

Adiponectin has been shown to act as an insulin sensitizer, yet the molecular mechanism underlying the cross-talk between the insulin and adiponectin signaling pathways remains largely unknown. The IRS-phosphatidylinositol (PI) 3-kinase pathway is the key insulin-

signaling pathway. Both IRS-1 to Akt and 2 atypical PKC isozymes act downstream of the PI3-kinase that plays an essential role in glucose uptake and GLUT4 translocation. Evidence supporting the input of Akt at the level of intracellular compartments includes migration of Akt/PKB to endomembranes containing GLUT4 in response to insulin (Sakamoto et al., 2000). PKC isoforms λ and ζ are downstream mediators of PI 3-kinase and their activation is required for insulin stimulation of glucose uptake, which involves translocation of the major insulin-responsive glucose transporter GLUT4 from intracellular sites to the cell membrane (Standaert et al., 1997). AMPK, which is not downstream of the PI 3-kinase, is a fuel-sensing enzyme that has been implicated in the regulation of glucose and lipid homeostasis and insulin sensitivity (Fisher et al., 2002; Iglesias et al., 2002). Adiponectin mediates the activation of AMPK, PPARα, and fatty acid oxidation in muscle or liver, thereby increasing glucose uptake and improving lipid metabolism (Yamauchi et al., 2003).

Pioglitazone did not increase IRS-1 (Tyr508), Akt, and PKCλ/ζ phosphorylation but enhanced AMPK (Thr172) phosphorylation under insulin stimulation (Fig. 7). It is implied that pioglitazone enhances insulin sensitivity through AMPK phosphorylation. It has been reported in several previous studies that TZDs or adiponectin increased the insulin sensitivity via AMPK phosphorylation in muscle cells (Fisher et al., 2002; Iglesias et al., 2002). It was theorized recently that adiponectin may sensitize insulin signaling by inhibiting S6K through an AMPK-dependent signaling pathway in muscle cells (Wang et al., 2007). Consequently, many studies were conducted on the effect of TZD or adiponectin on AMPK signaling pathway in the muscle but only few studies were performed in adipocytes. In a limited study, globular adiponectin significantly increased insulin-stimulated glucose uptake in a dose-dependent manner in addition to its enhancement of AMPK activity in primary adipocytes (Wu et al., 2003). It has been reported that targeted disruption of AdipoR1 in the liver resulted in the abrogation of adiponectin-induced AMPK activation, whereas that of AdipoR2 resulted in decreased activity of PPARα signaling pathways (Yamauchi et al., 2007). As for this dissociation, it is possible that downstream of AdipoR1/AdipoR2-signaling is different from that in insulin-targeted organs.

However, in another previous report, 5-aminoimidazole-4-carboxamide ribonucleoside (AICAR), a compound that activates AMPK, inhibited insulin-stimulated glucose transport in 3T3-L1 (Salt et al., 2000). Moreover, AMPK activation is essential for AICAR-induced glucose transport in the skeletal muscle but not in 3T3-L1 adipocytes (Sakoda et al., 2002). It has been reported that AICAR significantly increased AMPK phosphorylation at Thr-172 but it did not increase AMPK enzyme activity or glucose uptake in primary rat adipocytes. This may potentially explain why AICAR has little effect on adipocyte glucose uptake (Wu et al., 2003).

Conclusion

In this study, we showed that pioglitazone increases AdipoR2 expression in 3T3-L1 adipocytes. We also showed that pioglitazone might increase insulin sensitivity via AdipoR2-mediated AMPK phosphorylation in 3T3-L1 adipocytes (Fig. 9).

Conflict of interest statement

None.

Acknowledgments

We are indebted to Yuko Ohashi, Emiko Seino, and Atsuko Hashimoto for excellent technical assistance. This work was supported in part by the Salt Science Research Foundation, No. 08C4 (H.S.), a Kanae Foundation for Life & Soci-Medical Science grant (H.S.), a Takeda Science Foundation grant (H.S.), and a Grant-in-Aid Scientific Research from the Ministry of Education, Culture, Sports, Science, and Technology (H.S.).

References

Auboeuf D, Rieusset J, Fajas L, Vallier P, Frering V, Riou JP, et al. Tissue distribution and quantification of the expression of mRNAs of peroxisome proliferator-activated receptors and liver X receptor-alpha in humans: no alteration in adipose tissue of obese and NIDDM patients. Diabetes 1997;46(8):1319–27.

Berg AH, Combs TP, Du X, Brownlee M, Scherer PE. The adipocyte-secreted protein Acrp30 enhances hepatic insulin action. Nat Med 2001;7(8):947–53.

Caminos JE, Nogueiras R, Gallego R, Bravo S, Tovar S, Garcia-Caballero T, et al. Expression and regulation of adiponectin and receptor in human and rat placenta. J Clin Endocrinol Metab 2005;90(7):4276–86.

Coletta DK, Sriwijitkamol A, Wajcberg E, Tantiwong P, Li M, Prentki M, et al. Pioglitazone stimulates AMP-activated protein kinase signalling and increases the expression of genes involved in adiponectin signalling, mitochondrial function and fat oxidation in human skeletal muscle in vivo: a randomised trial. Diabetologia 2009;52(4):723–32.

Dormandy JA, Charbonnel B, Eckland DJ, Erdmann E, Massi-Benedetti M, Moules IK, et al. Secondary prevention of macrovascular events in patients with type 2 diabetes in the PROactive Study (PROspective pioglitAzone Clinical Trial In macroVascular Events): a randomised controlled trial. Lancet 2005;366(9493):1279–89.

Fisher JS, Gao J, Han DH, Holloszy JO, Nolte LA. Activation of AMP kinase enhances sensitivity of muscle glucose transport to insulin. Am J Physiol Endocrinol Metab 2002;282(1):E18–23.

Flier JS. Obesity wars: molecular progress confronts an expanding epidemic. Cell 2004;116(2):337–50.

Fruebis J, Tsao TS, Javorschi S, Ebbets-Reed D, Erickson MR, Yen FT, et al. Proteolytic cleavage product of 30-kDa adipocyte complement-related protein increases fatty acid oxidation in muscle and causes weight loss in mice. Proc Natl Acad Sci U S A 2001;98(4):2005–10.

Hirose H, Kawai T, Yamamoto Y, Taniyama M, Tomita M, Matsubara K, et al. Effects of pioglitazone on metabolic parameters, body fat distribution, and serum adiponectin levels in Japanese male patients with type 2 diabetes. Metabolism 2002;51(3):314–7.

Hotta K, Funahashi T, Bodkin NL, Ortmeyer HK, Arita Y, Hansen BC, et al. Circulating concentrations of the adipocyte protein adiponectin are decreased in parallel with reduced insulin sensitivity during the progression to type 2 diabetes in rhesus monkeys. Diabetes 2001;50(5):1126–33.

Hu E, Liang P, Spiegelman BM. AdipoQ is a novel adipose-specific gene dysregulated in obesity. J Biol Chem 1996;271(18):10697–703.

Iglesias MA, Ye JM, Frangioudakis G, Saha AK, Tomas E, Ruderman NB, et al. AICAR administration causes an apparent enhancement of muscle and liver insulin action in insulin-resistant high-fat-fed rats. Diabetes 2002;51(10):2886–94.

Lehmann JM, Moore LB, Smith-Oliver TA, Wilkison WO, Willson TM, Kliewer SA. An antidiabetic thiazolidinedione is a high affinity ligand for peroxisome proliferator-activated receptor gamma (PPAR gamma). J Biol Chem 1995;270(22):12953–6.

Li W, Tonelli J, Kishore P, Owen R, Goodman E, Scherer PE, et al. Insulin-sensitizing effects of thiazolidinediones are not linked to adiponectin receptor expression in human fat or muscle. Am J Physiol Endocrinol Metab 2007;292(5):E1301–7.

Maeda K, Okubo K, Shimomura I, Funahashi T, Matsuzawa Y, Matsubara K. cDNA cloning and expression of a novel adipose specific collagen-like factor, apM1 (AdiPose Most abundant Gene transcript 1). Biochem Biophys Res Commun 1996;221(2):286–9.

Nakano Y, Tobe T, Choi-Miura NH, Mazda T, Tomita M. Isolation and characterization of GBP28, a novel gelatin-binding protein purified from human plasma. J Biochem (Tokyo) 1996;120(4):803–12.

Nguyen MT, Satoh H, Favelyukis S, Babendure JL, Imamura T, Sbodio JI, et al. JNK and tumor necrosis factor-alpha mediate free fatty acid-induced insulin resistance in 3T3-L1 adipocytes. J Biol Chem 2005;280(42):35361–71.

Okuno A, Tamemoto H, Tobe K, Ueki K, Mori Y, Iwamoto K, et al. Troglitazone increases the number of small adipocytes without the change of white adipose tissue mass in obese Zucker rats. J Clin Invest 1998;101(6):1354–61.

Olefsky JM. Treatment of insulin resistance with peroxisome proliferator-activated receptor gamma agonists. J Clin Invest 2000;106(4):467–72.

Sakamoto J, Kimura H, Moriyama S, Odaka H, Momose Y, Sugiyama Y, et al. Activation of human peroxisome proliferator-activated receptor (PPAR) subtypes by pioglitazone. Biochem Biophys Res Commun 2000;278(3):704–11.

Sakoda H, Ogihara T, Anai M, Fujishiro M, Ono H, Onishi Y, et al. Activation of AMPK is essential for AICAR-induced glucose uptake by skeletal muscle but not adipocytes. Am J Physiol Endocrinol Metab 2002;282(6):E1239–44.

Salt IP, Connell JM, Gould GW. 5-Aminoimidazole-4-carboxamide ribonucleoside (AICAR) inhibits insulin-stimulated glucose transport in 3T3-L1 adipocytes. Diabetes 2000;49(10):1649–56.

Saltiel AR, Kahn CR. Insulin signalling and the regulation of glucose and lipid metabolism. Nature 2001;414(6865):799–806.

Satoh H, Nguyen MT, Miles PD, Imamura T, Usui I, Olefsky JM. Adenovirus-mediated chronic "hyper-resistinemia" leads to in vivo insulin resistance in normal rats. J Clin Invest 2004;114(2):224–31.

Satoh H, Nguyen MT, Trujillo M, Imamura T, Usui I, Scherer PE, et al. Adenovirus-mediated adiponectin expression augments skeletal muscle insulin sensitivity in male Wistar rats. Diabetes 2005;54(5):1304–13.

Scherer PE. Adipose tissue: from lipid storage compartment to endocrine organ. Diabetes 2006;55(6):1537–45.
Scherer PE, Williams S, Fogliano M, Baldini G, Lodish HF. A novel serum protein similar to C1q, produced exclusively in adipocytes. J Biol Chem 1995;270(45): 26746–9.
Shimizu A, Takamura T, Matsuzawa N, Nakamura S, Nabemoto S, Takeshita Y, et al. Regulation of adiponectin receptor expression in human liver and a hepatocyte cell line. Metabolism 2007;56(11):1478–85.
Spiegelman BM. PPAR-gamma: adipogenic regulator and thiazolidinedione receptor. Diabetes 1998;47(4):507–14.
Standaert ML, Galloway L, Karnam P, Bandyopadhyay G, Moscat J, Farese RV. Protein kinase C-zeta as a downstream effector of phosphatidylinositol 3-kinase during insulin stimulation in rat adipocytes. Potential role in glucose transport. J Biol Chem 1997;272(48):30075–82.
Tan GD, Debard C, Funahashi T, Humphreys SM, Matsuzawa Y, Frayn KN, et al. Changes in adiponectin receptor expression in muscle and adipose tissue of type 2 diabetic patients during rosiglitazone therapy. Diabetologia 2005;48(8):1585–9.
Tsuchida A, Yamauchi T, Ito Y, Hada Y, Maki T, Takekawa S, et al. Insulin/Foxo1 pathway regulates expression levels of adiponectin receptors and adiponectin sensitivity. J Biol Chem 2004;279(29):30817–22.
Tsuchida A, Yamauchi T, Takekawa S, Hada Y, Ito Y, Maki T, et al. Peroxisome proliferator-activated receptor (PPAR)alpha activation increases adiponectin receptors and reduces obesity-related inflammation in adipose tissue: comparison of activation of PPARalpha, PPARgamma, and their combination. Diabetes 2005;54(12):3358–70.
Tzameli I, Fang H, Ollero M, Shi H, Hamm JK, Kievit P, et al. Regulated production of a peroxisome proliferator-activated receptor-gamma ligand during an early phase of adipocyte differentiation in 3T3-L1 adipocytes. J Biol Chem 2004;279(34):36093–102.
Vaxillaire M, Dechaume A, Vasseur-Delannoy V, Lahmidi S, Vatin V, Lepretre F, et al. Genetic analysis of ADIPOR1 and ADIPOR2 candidate polymorphisms for type 2 diabetes in the Caucasian population. Diabetes 2006;55(3):856–61.
Wang C, Mao X, Wang L, Liu M, Wetzel MD, Guan KL, et al. Adiponectin sensitizes insulin signaling by reducing p70 S6 kinase-mediated serine phosphorylation of IRS-1. J Biol Chem 2007;282(11):7991–6.
Wu X, Motoshima H, Mahadev K, Stalker TJ, Scalia R, Goldstein BJ. Involvement of AMP-activated protein kinase in glucose uptake stimulated by the globular domain of adiponectin in primary rat adipocytes. Diabetes 2003;52(6):1355–63.
Yamauchi T, Kamon J, Waki H, Terauchi Y, Kubota N, Hara K, et al. The fat-derived hormone adiponectin reverses insulin resistance associated with both lipoatrophy and obesity. Nat Med 2001;7(8):941–6.
Yamauchi T, Kamon J, Minokoshi Y, Ito Y, Waki H, Uchida S, et al. Adiponectin stimulates glucose utilization and fatty-acid oxidation by activating AMP-activated protein kinase. Nat Med 2002;8(11):1288–95.
Yamauchi T, Kamon J, Ito Y, Tsuchida A, Yokomizo T, Kita S, et al. Cloning of adiponectin receptors that mediate antidiabetic metabolic effects. Nature 2003;423(6941): 762–9.
Yamauchi T, Nio Y, Maki T, Kobayashi M, Takazawa T, Iwabu M, et al. Targeted disruption of AdipoR1 and AdipoR2 causes abrogation of adiponectin binding and metabolic actions. Nat Med 2007;13(3):332–9.

糖尿病における腎臓病・CKDの診断・検査法

小川 大輔　　横野 博史

慢性腎臓病 chronic kidney disease（CKD）は，2002年に米国腎臓財団 National Kidney Foundation（NKF）のK DOQI（Kidney Disease Outcomes Quality Initiative）診療ガイドラインにおいて提唱された疾患概念である[1]．その後，世界的に受け入れられ，CKDの早期発見，早期対策・治療の重要性が認識されている．CKDは末期腎不全となり，透析療法あるいは腎移植が必要になるだけでなく，その進行の過程で脳梗塞，狭心症・心筋梗塞，末梢動脈疾患などさまざまな心血管疾患 cardiovascular disease（CVD）を引き起こす危険が大きい（**図8-1**）．糖尿病腎症はCKDの代表疾患であるが，糖尿病患者に腎硬化症や糸球体腎炎が合併する場合もある．本章では，糖尿病における腎臓病，CKDの診断・検査法，腎臓専門医との連携について概説する．

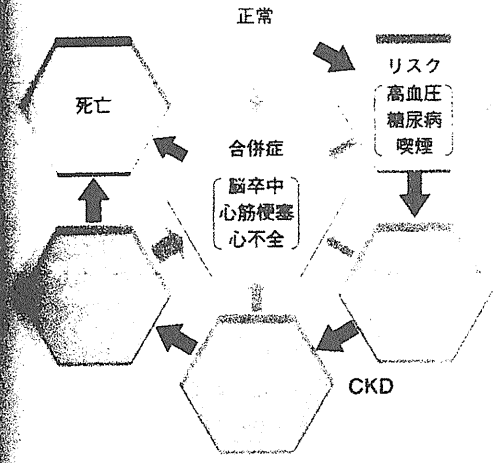

［日本腎臓学会 編：CKD診療ガイド2009，p.19を一部改変］

図8-1　CKDの発症と進行の概念

糸球体濾過量を評価する検査

糸球体濾過量 glomerular filtration rate（GFR）を評価する検査方法としては**表8-1**に示す通り，クレアチニンクリアランス creatinine clearance（Ccr），推算糸球体濾過量 estimated glomerular filtration rate（eGFR），イヌリンクリアランス，シスタチンCなどがある．

日常臨床の場において24時間蓄尿を行い，尿量，血清クレアチニン（Cr）値，尿CrからCcrを算出しGFRを推定する方法である．蓄尿の不正確さなどの問題もあるが，同時に1日尿タンパク量や1日食塩推定摂取量，1日タンパク質推定摂取量などを算出することができ，診療上有用な多くの情報が得られる．尿細管からのCr分泌のため，GFRより30%程度大きい値をとることに

表8-1　腎機能の評価

クレアチニンクリアランス creatinine clearance（Ccr） Ccr（mL/分）＝尿中Cr（mg/dL）×尿量（mL/日）/血清Cr（mg/dL）×1,440（分/日）
推算糸球体濾過量 estimated glomerular filtration rate（eGFR） eGFR（mL/分/1.73 m^2）＝ $194 \times Cr^{-1.094} \times Age^{-0.287}$（女性はこれに×0.739）
イヌリンクリアランス
シスタチンC

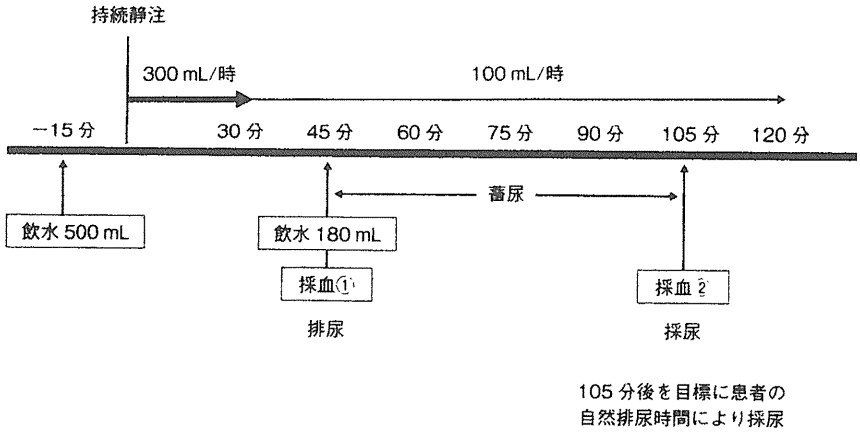

図 8-2　イヌリンクリアランス測定法（簡易法）

留意する必要がある．

2）eGFR（推算糸球体濾過量）

血清 Cr，年齢，性別から簡便に GFR を推算する式が，日本腎臓学会より発表された[2]．eGFR は 24 時間蓄尿を必要としないため，非常に簡便な腎機能の指標である．今後，この式をもとに多くの臨床・疫学研究が進んでいくものと思われる．

3）イヌリンクリアランス

イヌリン（イヌリード®注）が認可されるまでは，24 時間 Ccr を測定して GFR が推定されていたが，2006 年に薬価収載されイヌリンクリアランスによる GFR 実測が可能となった．**図 8-2** に示すように煩雑であることから，日常臨床では上記の eGFR あるいは Ccr を用い，腎生検施行症例や腎移植ドナーなど正確な腎機能評価が必要な症例にはイヌリンクリアランスを用いる．

4）シスタチン C

シスタチン C は分子量 13,000 の低分子タンパクであり，全身の有核細胞から一定の割合で産生される．糸球体で濾過された後，ほとんどが近位尿細管で再吸収・分解されるので，血中濃度は GFR に依存している．シスタチン C は血清 Cr に比べると，年齢や性別に影響されず腎機能以外の影響を受けにくい．また，血清 Cr が増加し い程度の腎機能低下でもシスタチン C は上 認めるという点が特徴であり，血清 Cr に代わ 腎機能マーカーとして注目されている．

表 8-2　CKD の定義

尿異常，画像診断，血液，病理で腎障害の存在が明ら (特にタンパク尿の存在が重要)
GFR < 60 mL/分/1.73m^2
，　のいずれか，または両方が 3 カ月以上持続する

出典：日本腎臓学会 編：CKD 診療ガイド2009

CKD の定義とステージ分類

CKD とは，**表 8-2** で定義される．すな GFR で表される腎機能の低下があるか，も は腎臓の障害を示唆する所見が慢性的に持 ものをすべて包括している．日常診療で CKD はタンパク尿と GFR < 60 mL 分 で診断する．

CKD の病期分類には，腎機能の評価指 る GFR を用いる．シンプルに病期がイメー きるように，ステージが 15 および 30 の 切られている．また，ステージ分類にお 植（transplantation）患者である場合に ステージ 5 で透析（dialysis）を行って には D をつけることで，病期をより明 ようにしている[3]（p.64, **表 9-2**）．

表 8-3　アルブミン（Alb）尿の分類

	24 時間蓄尿 Alb（mg/24 時間）	夜間蓄尿 Alb（mg/分）	随時尿 Alb/Cr 比（ACR）（mg/g）
正常	＜15	＜10	＜10
正常高値	15～＜30	10～＜20	10～＜30
微量アルブミン尿	30～＜300	20～＜200	30～＜300
顕性アルブミン尿	≧300	≧200	≧300

出典：日本糖尿病学会・日本腎臓学会糖尿病性腎症合同委員会 編：糖尿病，48：757-759. 2005.

微量アルブミン尿検査の施行法とその有用性

随時尿の検査では起立性タンパク尿を除外するために一度は早朝第一尿で検査する．尿中アルブミン定量と尿中 Cr 濃度の測定を行い，尿中アルブミンと Cr の比を算出し，mg/gCr で表す．あるいは 24 時間蓄尿もしくは時間尿の採取を行い，あるいは時間あたりのアルブミン/タンパク尿中排泄量を定量する．

わが国の微量アルブミン尿の診断に関して，日本糖尿病学会・日本腎臓学会糖尿病性腎症合同委員会より糖尿病腎症の診断基準が作成されている（表 8-3）．微量アルブミン尿の存在は，早期糖尿病腎症の診断にきわめて重要である．早期の糖尿病腎症は試験紙法でタンパク尿が陰性のことが多く，アルブミン尿を測定し微量アルブミン尿の有無を確認する必要がある．

糖尿病患者で見逃してはいけない症状や臨床所見

タンパク尿が軽度の場合には症状はない．タンパク尿が高度となり，血清タンパク濃度が低下すると下腿浮腫，胸腹水貯留といった溢水症状が出現する．特に糖尿病腎症による腎不全患者では，しばしばネフローゼとなり体内の水分貯留傾向をおこしやすい．また腎不全が高度となると，吐き気や食欲低下などの尿毒症症状が出現する．

検査所見では，腎不全が進行すると血清 Cr のほか，尿素窒素，尿酸，K が上昇する．また，腎機能の低下に伴い貧血（腎性貧血）を認める．腎性貧血では，鉄欠乏性貧血と異なりエリスロポエチンの上昇が認められないという特徴がある．

糖尿病腎症とそのほかの腎疾患の合併や鑑別について

一般に糖尿病を発症し，おおまかに約 5 年で神経障害，約 10 年で網膜症，約 15 年で腎症を発症するといわれている[1]（p.148，図 8-3）．糖尿病腎症の診断および経過の把握には，タンパク尿，腎機能，腎組織所見を用いる．腎症の程度を把握するためには腎組織検査が最も確実な方法であるが，日常臨床の場では全例に腎生検を施行することは難しく，タンパク尿と腎機能の面から腎症の経過を把握する．

タンパク尿や腎機能低下を認める糖尿病患者で，糖尿病の罹病期間が短く，神経障害や網膜症も認めない場合は，糖尿病腎症によるものは考えにくく，他の腎疾患を考慮する．罹病期間の短い糖尿病患者の急激な腎機能低下や浮腫の出現をみたら，糖尿病腎症ではなく他の糸球体腎炎の合併を考慮し，積極的に腎生検を行う必要がある．

腎臓専門医へ患者を紹介すべき基準

上述のように，腎生検が必要となる場合は腎臓専門医にコンサルトしなくてはいけない．具体的な基準としては，試験紙法で 2+ 以上の尿タンパク，または 0.5 g/gCr（または g/日）以上の尿タンパクを呈する場合，あるいは 0.5 g/gCr（または g/日）未満の尿タンパクであっても血尿を伴

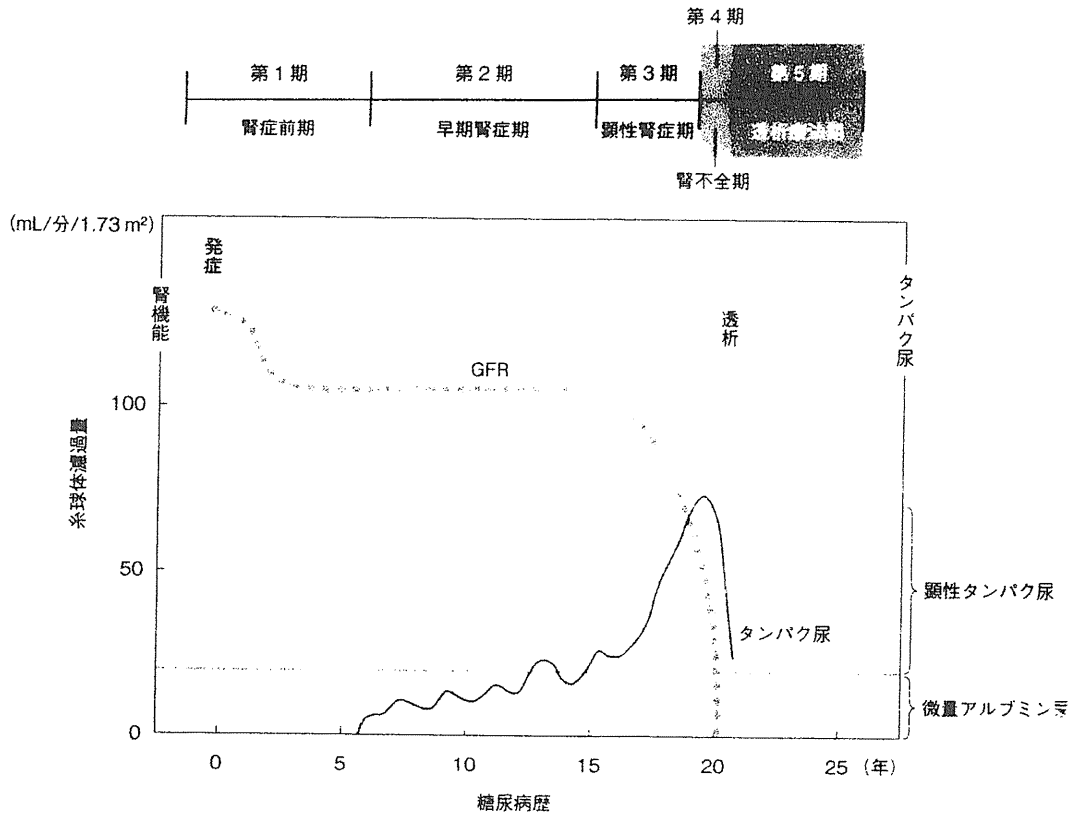

[横野博史 編：わかる糖尿病性腎症, p.43-44, 2002 を一部改変]

図 8-3 糖尿病腎症の臨床経過

表 8-4 CKD における腎生検の適応*

尿タンパクのみ陽性の場合	尿タンパクが 0.5 g/日以上，もしくは 0.5 g/g Cr 以上
尿タンパク，尿潜血ともに陽性の場合	尿タンパクが 0.5 g/日以下，もしくは 0.5 g/g Cr 以下でも考慮
ネフローゼ症候群の場合	積極的に施行
尿潜血のみ陽性の場合	尿沈渣に変形赤血球が多く存在する場合や病的円柱を認める場合などに考慮

＊いずれの場合にも糖尿病患者においては慎重に考慮すべきである．

出典：日本腎臓学会 編：エビデンスに基づく CKD 診療ガイドライン2009, p.8.

う場合は糸球体疾患の可能性があるため，腎生検を含めた精査を考慮する必要がある[5]（表 8-4）．また，急激な尿タンパクの増加や急激な GFR 低下がみられる場合にも紹介すべきである．

〈参考文献〉

1) National Kidney Foundation：K DOQI clinical practice guidelines for chronic kidney disease：evaluation, classification and stratification. Am J Kidney Dis. 39：S1-266, 2002.
2) Matsuo S, et al：Revised equations for estimated GFR from serum creatinine in Japan. Am J Kidney Dis. 53：982-992, 2009.
3) 日本腎臓学会 編：CKD診療ガイド2009. p.12-13. 東京医学社. 2009.
4) 横野博史 編：わかる糖尿病性腎症. p.43-44. 診断と治療社. 2002.
5) 日本腎臓学会 編：エビデンスに基づくCKD診療ガイドライン 2009. p.8. 東京医学社. 2009.

Hindawi Publishing Corporation
Experimental Diabetes Research
Volume 2011, Article ID 534872, 8 pages
doi:10.1155/2011/534872

Research Article

High Glucose Increases Metallothionein Expression in Renal Proximal Tubular Epithelial Cells

Daisuke Ogawa,[1,2] Masato Asanuma,[3] Ikuko Miyazaki,[3] Hiromi Tachibana,[1] Jun Wada,[1] Norio Sogawa,[4] Takeshi Sugaya,[5] Shinji Kitamura,[1] Yohei Maeshima,[1] Kenichi Shikata,[1,6] and Hirofumi Makino[1]

[1] *Department of Medicine and Clinical Science, Okayama University Graduate School of Medicine, Dentistry and Pharmaceutical Sciences, Okayama 700-8558, Japan*
[2] *Department of Diabetic Nephropathy, Okayama University Graduate School of Medicine, Dentistry and Pharmaceutical Sciences, Okayama 700-8558, Japan*
[3] *Department of Brain Science, Okayama University Graduate School of Medicine, Dentistry and Pharmaceutical Sciences, Okayama 700-8558, Japan*
[4] *Department of Dental Pharmacology, Okayama University Graduate School of Medicine, Dentistry and Pharmaceutical Sciences, Okayama 700-8558, Japan*
[5] *CMIC Company, Ltd., Tokyo 113-0034, Japan*
[6] *Center for Innovative Clinical Medicine, Okayama University Hospital, Okayama 700-8558, Japan*

Correspondence should be addressed to Daisuke Ogawa, daiogawa@md.okayama-u.ac.jp

Received 25 May 2011; Revised 25 July 2011; Accepted 31 July 2011

Academic Editor: Yasuhiko Tomino

Metallothionein (MT) is an intracellular metal-binding, cysteine-rich protein, and is a potent antioxidant that protects cells and tissues from oxidative stress. Although the major isoforms MT-1 and -2 (MT-1/-2) are highly inducible in many tissues, the distribution and role of MT-1/-2 in diabetic nephropathy are poorly understood. In this study, diabetes was induced in adult male rats by streptozotocin, and renal tissues were stained with antibodies for MT-1/-2. MT-1/-2 expression was also evaluated in mProx24 cells, a mouse renal proximal tubular epithelial cell line, stimulated with high glucose medium and pretreated with the antioxidant vitamin E. MT-1/-2 expression was gradually and dramatically increased, mainly in the proximal tubular epithelial cells and to a lesser extent in the podocytes in diabetic rats, but was hardly observed in control rats. MT-1/-2 expression was also increased by high glucose stimulation in mProx24 cells. Because the induction of MT was suppressed by pretreatment with vitamin E, the expression of MT-1/-2 is induced, at least in part, by high glucose-induced oxidative stress. These observations suggest that MT-1/-2 is induced in renal proximal tubular epithelial cells as an antioxidant to protect the kidney from oxidative stress, and may offer a novel therapeutic target against diabetic nephropathy.

1. Introduction

Diabetic nephropathy is a leading cause of end-stage renal disease, and many mechanisms have been proposed to explain the pathogenesis of renal injury in diabetes [1]. Recent studies have shown that hyperglycemia may induce oxidative stress by increasing reactive oxygen species (ROS) generation in the diabetic kidney [2–4] and that overexpression of the antioxidant superoxide dismutase 1 attenuated diabetic nephropathy in streptozotocin (STZ)-induced and *db*/*db* diabetic mice [5, 6]. Therefore, ROS could be an important mediator of diabetic nephropathy, and protection from ROS might offer a valuable therapeutic strategy to treat diabetic nephropathy.

Metallothionein (MT) is an intracellular metal-binding protein with a low-molecular mass (6-7 kDa) and a high cysteine content (20 of 61-62 amino acids). Its major isoforms, MT-1 and -2 (MT-1/-2), are widely distributed

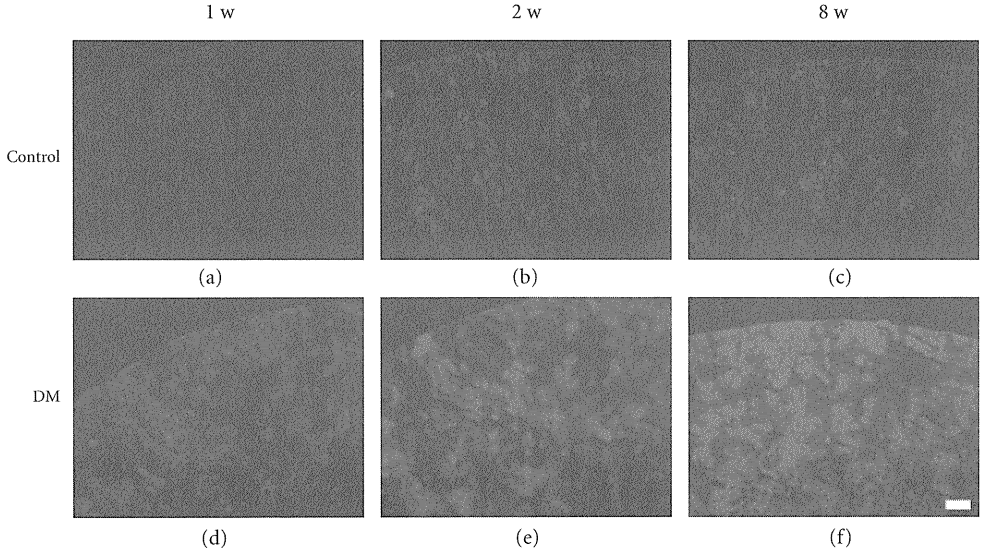

FIGURE 1: MT-1/-2 expression in the kidney. Diabetes was induced by injection of streptozotocin, and kidneys were obtained at 1 (a and d), 2 (b and e), or 8 (c and f) weeks after inducing diabetes. Immunofluorescent staining was performed as described in *Materials and Methods*. MT was strongly expressed in the renal cortex of diabetic rats (d, e, f) and hardly expressed in control rats (a, b, c). The expression of MT-1/-2 was greater at week 8 than at weeks 1 and 2 after diabetes induction. Scale bar: 100 μm.

throughout the body [7, 8]. Since MT-1/-2 expression is significantly upregulated by overload of essential trace metals (e.g., Zn and Cu), it plays an important role in heavy metal detoxification and essential metal homeostasis [9, 10]. In addition, MTs have been shown to act as nonspecific free radical scavengers [11, 12], suggesting that they exert antioxidant activities in various diseases, including diabetic nephropathy.

We and other investigators have demonstrated that MTs have neuroprotective effects in mouse models of Parkinson's disease [13–15]. In contrast, the role of MTs in the pathogenesis of diabetic nephropathy is poorly understood. Several studies reported that renal expression of MT is increased in STZ-induced diabetic rats [16], diabetic BB rats [17], and *ob*/*ob* diabetic mice [18]. However, the distribution of MTs in the diabetic kidney and the mechanisms by which MTs are induced in diabetes are poorly understood. Therefore, in the present study, we investigated the expression and localization of MT-1/-2 during the development of diabetic nephropathy and explored the mechanism by which MT-1/-2 expression was induced by high glucose in the kidney.

2. Materials and Methods

2.1. Experimental Protocol. Male Sprague Dawley rats were purchased from Charles River (Yokohama, Japan). Five-week-old rats were divided into two groups: (1) nondiabetic control rats (control; $n = 6$) and (2) STZ-induced diabetic rats (DM; $n = 6$). Diabetes was induced by peritoneal injection of 200 mg/kg STZ (Sigma-Aldrich Corp., MO) in citrate buffer (pH 4.5). Blood glucose was measured by the glucose oxidase method at 3 days after STZ injection and only rats with blood glucose concentrations >16 mmol/L were used in the study. All rats had free access to standard diet and tap water. All procedures were performed according to the Guidelines for Animal Experiments at Okayama University Medical School, Japanese Government Animal Protection and Management Law (No. 105) and the Japanese Government Notification on Feeding and Safekeeping of Animals (No. 6). Rats were sacrificed at 1, 2, or 8 weeks after inducing diabetes. We measured body weight, hemoglobin A1c (HbA1c), and 24-h urinary albumin excretion (UAE) at 1, 2, and 8 weeks. The kidneys were removed, weighed, and fixed in 10% formalin for periodic acid—methenamine silver (PAM) staining, and parts of the remaining tissues were embedded in optimal cutting temperature compound (Sakura Finetechnical, Tokyo, Japan) and frozen immediately in acetone cooled on dry ice.

2.2. Immunofluorescent Staining of MT-1/-2 in Rat Kidney. Immunofluorescent staining was performed as previously described [19]. Renal expression of MT-1/-2 was detected using mouse anti-MT-1/-2 antibody (Dako, Carpinteria, CA) followed by Alexa Fluor 594 goat anti-mouse IgG (Invitrogen, Carlsbad, CA). To determine whether MT-1/-2 was localized in podocytes or proximal tubular epithelial cells, the sections were counterstained with guinea pig antinephrin antibody (Fitzgerald, Concord, MA) or rabbit antiaquaporin 1 antibody (Millipore, Billerica, MA), followed by Alexa Fluor 488 goat anti-guinea pig IgG or anti-rabbit IgG (Invitrogen), respectively. Fluorescence images were obtained using a fluorescence microscope (BX51; Olympus, Tokyo, Japan).

2.3. Cell Culture and Treatment. mProx24 cells, a murine renal proximal tubular epithelial cell line derived from